Piperazine Based Metallomacrocyclic Dithiocarbamate Complexes: Synthesis, Characterization and Their Photophysical Properties

Abstract

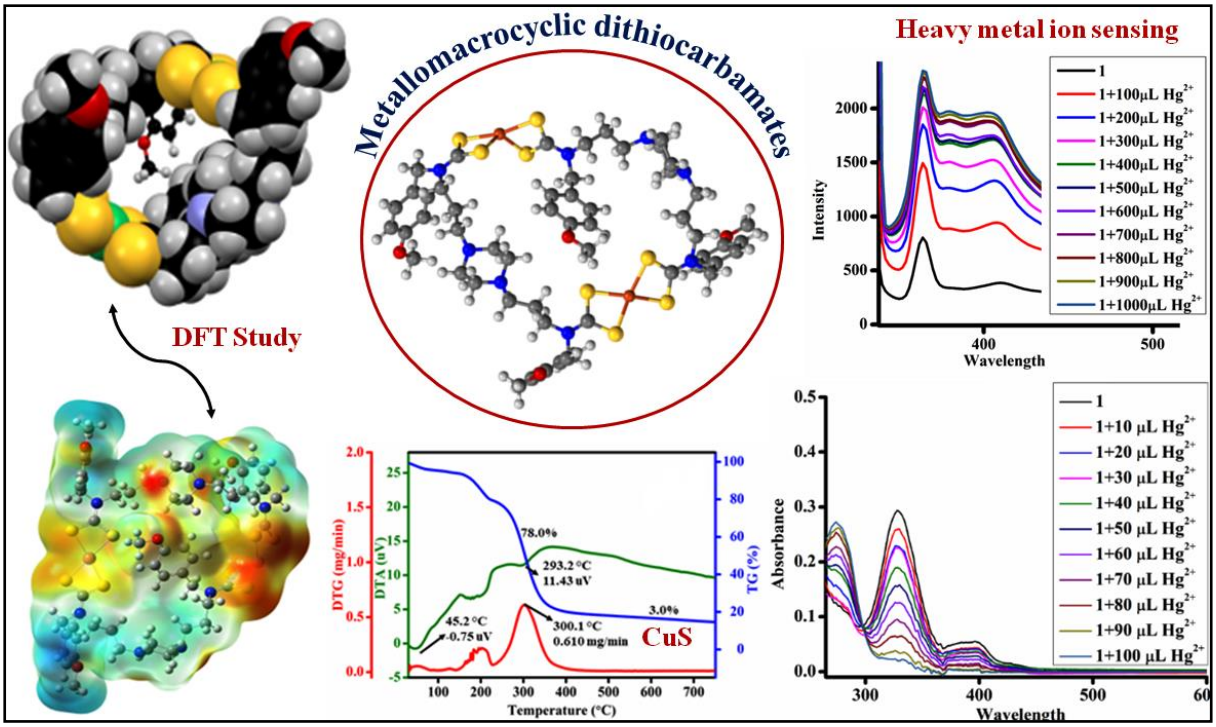

Two novel secondary diamines *viz.* *N,N'*-bis{3-(*p*-methoxybenzylamino)propyl}piperazine (**H_2L^5**) and *N,N'*-bis{3-(p-chlorobenzylamino)propyl}piperazine (**H_2L^6**) holding *N,N'*-bispropylpiperazine linkers have been prepared in chapter 2 and subsequently used to derive a new series of *N,N'*-bis(3-dithiocarbamatopropyl) piperazine bridged metallomacrocyclic complexes $[M(II)_2$-μ^2-bis-$\{(\kappa^2S,S$-$S_2CN(R)C_3H_6)_2$piperazine$\}]$ wherein R = *p*-methoxybenzyl, M = Ni(II) **13**, Cu(II) **14**, Zn(II) **15**; R = *p*-chlorobenzyl, M = Ni(II) **16**, Cu(II) **17**, Zn(II) **18**. The formation and purity of all the binuclear metallomacrocyclic dithiocarbamate complexes were verified by microanalysis and standard spectroscopic methods such as HRMS, NMR, IR and UV-visible absorption spectroscopy and corroborated by density functional theory calculations. The experimental (magnetic moment and UV-visible) and theoretical calculations suggest square planar/distorted square planar environment around nickel(II)/ copper(II) and tetrahedral/distorted tetrahedral environment around zinc(II) centres in **13-18**. Thermogravimetric study was carried out on **13-18** to study

their thermal stability and degradation behaviour. Interestingly, TG curves of compounds **14**, **15** and **17** gave a stable residual mass corresponding to corresponding metal sulphides (MS) and suggest their potential utility as single source precursors for the synthesis of high purity MS nanoparticle as a new class of resources for energy conversion and/or storage applications due to their low cost. Notably, the calculated HOMO-LUMO gaps (1.19-1.33 eV) for Cu(II)-dithiocarbamate **14** and **17** indicates their semiconducting nature. The potentials of these binuclear metallomacrocycles as a molecular probe for optical sensing of environmentally hazardous heavy metal ions *ca* Pb(II), Cd(II) and Hg(II) were further examined by using UV-visible and fluorescence spectroscopies.

5.1 Introduction

The detection and isolation of environmentally hazardous heavy metal ions *viz.* Cd^{2+}, Hg^{2+} and Pb^{2+} causing a serious health hazard has became a thrust area of current research.[1]

Reports suggest that even at very low concentrations (15 ppb), Pb^{2+} is directly impounded by cells from the environment and interferes with numerous biological processes that ultimately result into neurological, cardiovascular, reproductive and developmental effects in humans.[2] Pb^{2+} is known to interact with proteins by either mimicking or antagonizing the physiological effects of divalent metals such as Ca^{2+} and Zn^{2+}. Like Pb^{2+}, Cd^{2+} is also toxic to cells due to interfering with Ca^{2+} and Zn^{2+}dependent processes. However, serious challenges[3] for expanding Cd^{2+} probes come from the very similar binding properties of Cd^{2+} and Zn^{2+} and thus, it remains difficult to advance selective probes for Cd^{2+} that do not interfere with Zn^{2+} under physiological conditions.[4] Moreover, detection of Hg^{2+} is of great importance due to its high toxicity, widespread distribution in the environment and its easy accumulation in organism through the food chain.[5]

The high-performance liquid chromatography (HPLC),[6] capillary electrophoresis,[7] potentiometric,[8] conductometric/electrochemical,[9] colorimetry,[10] chromogenic stain, dyes[11] and fluorescence[1, 5] has long been used to visualize the metals of interest, however additional approaches are required to envision the metal of concerns, particularly in the complex environment of multiple metals. Although, instrumental techniques often provide direct and quantitative information about metal ions, however such techniques are not well-suited for their quick detection in the field or for in vivo studies of heavy metal ion biology and toxicology.

Synthetic chemists have undertaken the challenge of design and synthesis of small-molecule metal ions sensor to overcome such problems. Several chemosensors for detecting

free Hg^{2+} and Pb^{2+} ions selectively have been reported by Professor Pandey *et al.*[12] and others that are emphasized in a comprehensive review article.[5] In the light of better thiophilicity of Hg^{2+} and Pb^{2+} ions over oxophilicity, a number of sulphur rich chemosensors have been developed for these ions to image HeLa cells as well as zebra fish.[13-14] In particular, histidine residues appended to a bipodal thiocarbamate scaffold (Hatai Hg-1) provide sulphur atoms as donors to increase selectivity for Hg^{2+}.[15]

Although, there are sensitive and selective chemosensors reported for the sensing and binding of heavy metal ions Pb^{2+}, Cd^{2+} and Hg^{2+}, however, the field continues to push for improved sensors to combat growing environmental pollution concerns. For instance, substituted organic macrocyclic compounds containing azacrown ethers,[16] calix[4]arene,[17] diazatetrathia-crown ether[18], cyclam,[19] dipyrrolylquinoxaline-bridged organic macrocycles,[20] and several other organic macrocyclic chelates[21] provide fluorescence turn-off and turn-on activity however, many of these probes have low selectivity for d^{10} metal ions over other divalent metal ions viz. Ni^{2+}, Cu^{2+} and Zn^{2+}.

Interestingly, several dinuclear/ mononuclear dithiocarbamates macrocycles[22] are reported by us and many other authors[23], however, they are either investigated for their potential in vitro-biological study or molecular recognition, anion receptors, ion-pair recognition in the sensing of gas storage, metal-sulphide nanoparticle synthesis. The investigations on metallomacrocyclic dithiocarbamate transition metal complexes based chemosensor probes for the detection of Pb^{2+}, Cd^{2+} and $Hg^{2+}$are in the embryonic stage. Surprisingly, such sulphur rich metallomacrocyclic dithiocarbamate complexes are not yet studied satisfactorily in the sensing and isolation of heavy metal ions Pb^{2+}, Cd^{2+} and Hg^{2+}, except Li^+, Na^+, K^+, Cs^+, neutral organic or anionic guest species such as halides, $H_2PO_4^-$, CH_3COO^- and $C_6H_5COO^-$. [24]

In the present work, Interesting potential applications of binuclear metallomacrocyclic dithiocarbamate complexes have encouraged us to synthesize a new series of metallomacrocyclic dithiocarbamate complexes [M(II)$_2$-μ^2-bis-{(κ^2*S*,*S*-$S_2CN(R)C_3H_6)_2$piperazine}] wherein R = *p*-methoxybenzyl, M = Ni(II) **13**, Cu(II) **14**, Zn(II) **15**; R = *p*-chlorobenzyl, M = Ni(II) **16**, Cu(II) **17**, Zn(II) **18**, holding bispropyl piperazine linkers. All the compounds were investigated for their potential small-molecule probes in the sensing of heavy metal ions viz. Pb(II), Cd(II) and Hg(II) by using UV-visible absorption and emission techniques. With keenness, the incorporation of the soft sulphur atoms and with their added features to show variable coordination number, geometry, oxidation state, color,

redox, electronic, steric and magnetic properties, in combination with functionalized organic ligands, these metallomacrocyclic dithiocarbamate complexes can be established as better small-molecule probe in the sensing and recovery of heavy metal ions through effective sensitivity, selectivity and binding affinity towards Pb(II), Cd(II) and Hg(II) heavy metal ions.

5.2 Experimental Section

5.2.1 Materials and Instrumentations

All the synthetic manipulations were performed in an open atmosphere. The solvents were of laboratory grade available at various commercial sources and distilled prior to use by following the standard procedures. 1,4-bis(3-aminopropyl)piperazine (>98%) (TCI Chemicals), potassium hydroxide (97%) (Fisher Scientific), carbon disulfide (99%) (Fisher Scientific), sodium borohydride (97%) (Fisher Scientific), metal acetates such as $Ni(OAc)_2 \cdot 4H_2O$, $Cu(OAc)_2 \cdot H_2O$, $Zn(OAc)_2 \cdot 2H_2O$ (98%) (all Merck), 4-methoxybenzaldehyde (98%), 4- chlorobenzaldehyde (98%) (Avra) were used as received. Ligand precursors N,N'-bis{3-(*p*-methoxybenzylamino)propyl}piperazine (**H_2L^5**) and N,N'-bis{3-(*p*-chlorobenzylamino)propyl}piperazine (**H_2L^6**) were synthesized following the literature procedure. The reaction and manipulations were performed at room temperature. Thin Layer Chromatography was performed on Merck 60 F254 aluminium-coated plates. Elemental analyses were performed on a Perkin-Elmer Series II CHNS Analyzer 2400. High resolution mass spectrometry (HR-MS) analysis was performed by using an instrument Waters, Synapt XS HDMS containing a separation module of UPLC Acquity H class series system under electro spray positive (ES+) ionization mode. FTIR (KBr pellets) spectra of the samples were recorded in the 4000–400 cm^{-1} range using a Bruker FTIR spectrometer. The NMR experiments were carried out on a Bruker AV-III 400 MHz spectrometer in spectrometer with $CDCl_3$ solvent and TMS as internal standard. UV-visible absorption and fluorescence spectra were recorded on a JASCO V-730 UV-visible and JASCO FP 8200 spectrophotometer, respectively. TGA/DTA plots were obtained using SII TG/DTA 6300 in flowing N_2 with a heating rate of 10 °C min^{-1}. The geometry of the molecules was optimized with the Gaussian 16 program and molecular orbitals were generated using GaussView 6.0 program.

5.2.2 Synthesis of Binuclear metallomacrocyclic dithiocarbamate complexes [M(II)$_2$-μ^2-bis-{(κ^2*S*,*S*-S$_2$CN(R)C$_3$H$_6$)$_2$piperazine}] wherein R = *p*-methoxy benzyl, M = Ni(II) 13, Cu(II) 14, Zn(II) 15; R = *p*-chlorobenzyl, M = Ni(II) 16, Cu(II) 17, Zn(II) 18

To a solution of 1 equivalent of diamine ligand *N,N'*-bis{3-(p-methoxybenzylamino)propyl}piperazine **H$_2$L^5** (0.44 g, 1 mmol) or *N,N'*-bis{3-(p-chlorobenzylamino)propyl}piperazine **H$_2$L^6** (0.45 g, 1 mmol) in acetonitrile, 2.1 equivalent potassium hydroxide (0.12 g, 2.1 mmol) was added and the reaction mixture was stirred for half an hour at room temperature. An excess of carbon disulphide (~10 mmol) was then added and the reaction mixture was continued to stir for further 8 hours at room temperature. During this time period, a change in colour from pale yellow to yellow was observed. To this reaction mixture, $Ni^{II}(C_2H_3O_2)_2.4H_2O$ (0.27 g, 1.1 mmol), $Cu^{II}(C_2H_3O_2)_2.H_2O$ (0.22 g, 1.1 mmol) or $Zn^{II}(C_2H_3O_2)_2.2H_2O$ (0.24 g, 1.1 mmol) was added and the stirring was continued for another 12 hours. The residue was filtered and washed several times by water followed by n-hexane. The residue was dried under high vacuum to yield the corresponding *N,N'*-bispropyl piperazine incorporated metallomacrocyclic dithiocarbamate complexes **13-18**. The compounds are taken for experimental study.

Table 1. Micro- and IR analysis data for complexes **13-18**.

Entry	Molecular Formula	Molecular Weight	Yield (%)	Melting/Dec. Point (°C)	Elemental Analysis % Found (calculated)				IR data (KBr disc) υ_{max}/cm^{-1}
					C	H	N	S	
13	$C_{56}H_{76}N_8Ni_2O_4S_8$	1299.14	78	122	51.82 (51.77)	5.97 (5.90)	8.68 (8.63)	19.80 (19.74)	3437(w), 2931(w), 2809(w), 2773(w), 1612(w), 1509(s), 1436(w), 1351(w), 1300(w), 1248(s), 1174(w), 1111(w), 1030(w), 985(w), 909(w), 814(w), 756(w), 617(w), 531(w)
14	$C_{56}H_{76}Cu_2N_8O_4S_8$	1308.85	66	144	51.45 (51.39)	5.92 (5.85)	8.63 (8.56)	19.71 (19.60)	3431(w), 2932(w), 2808(w), 2772(w), 1610(s), 1583(w), 1511(vs), 1460(w), 1351(w), 1300(w), 1248(s), 1211(w), 1174(s), 1110(w), 1088(w), 1030(s), 971(w), 812(w), 754(w), 709(w), 618(w), 530(w), 448(w)
15	$C_{56}H_{76}N_8O_4S_8Zn_2$	1312.52	63	164	51.32 (51.25)	5.87 (5.84)	8.58 (8.54)	19.58 (19.54)	3435(w), 2933(s), 2811(w), 2774(w), 1610(s), 1583(w), 1512(vs), 1485(w), 1415(w), 1352(w), 1301(w), 1248(vs), 1215(w), 1175(s), 1111(w), 1089(w), 1031(s), 970(w), 908(w), 843(w), 813(s), 756(w), 622(w), 533(w), 448(w)
16	$C_{52}H_{64}Cl_4N_8Ni_2S_8$	1316.81	73	172	47.49 (47.43)	4.93 (4.90)	8.57 (8.51)	19.54 (19.48)	3439(w), 2936(w), 2810(w), 1626(w), 1551(w), 1494(vs), 1431(w), 1406(w), 1349(w), 1300(w), 1275(w), 1216(w), 1163(w), 1090(w), 1014(s), 798(w), 755(w), 688(w), 606(w), 483(w)
17	$C_{52}H_{64}Cl_4Cu_2N_8S_8$	1326.51	61	140	47.14 (47.08)	4.89 (4.86)	8.49 (8.45)	19.39 (19.33)	3427(w), 2937(w), 2809(s), 2773(w), 1655(w), 1491(vs), 1429(w), 1405(w), 1350(w), 1300(w), 1274(w), 1214(s), 1164(w), 1090(s), 1014(s), 978(w), 840(w), 798(s), 751(w), 666(w), 606(w), 482(w), 430(w)
18	$C_{52}H_{64}Cl_4N_8S_8Zn_2$	1330.18	58	158	47.02 (46.95)	4.88 (4.85)	8.43 (8.42)	19.37 (19.28)	3442(w), 2939(w), 2813(w), 2775(w), 1641(w), 1490(vs), 1426(w), 1405(s), 1350(w), 1301(w), 1274(w), 1214(s), 1165(w), 1091(s), 1014(s), 972(w), 912(w), 841(w), 819(w), 798(s), 754(s), 665(w), 604(w), 483(w)

Table 2. NMR spectral data for complexes **13, 15, 16, 18**.

Entry	NMR Data (ppm)	
	^{1}H NMR ($CDCl_3$)	**^{13}C NMR ($CDCl_3$)**
13	7.29-6.88 (m, 16H, -*Ph*), 4.73 (s, 8H, PhC*H*$_2$), 3.83 (s, 12H, -OC*H*$_3$), 3.51 (s, 8H, S_2CNCH_2), 2.39-2.29 (m, 24H, NC*H*$_2$), 1.78 (s, 8H, NCH_2CH_2)	207.4 (-*NCS*$_2$), 159.6, 129.9, 129.7, 126.3, 114.3, 55.4, 54.9, 52.9, 51.6, 46.5, 24.0
15	7.33-6.88 (m, 16H, *Ph*), 5.09 (s, 8H, PhC*H*$_2$), 3.81 (s, 12H, -OC*H*$_3$), 3.79 (s, 8H, S_2CNCH_2 *merged with methoxy signal*), 2.36-2.34 (m, 24H, NC*H*$_2$) 1.94 (s, 8H, NCH_2CH_2)	204.3 (-*NCS*$_2$), 159.5, 129.4, 127.1, 114.2, 57.3, 55.3, 55.2, 53.0, 51.6, 23.8
16	7.78-7.22- (m, 16H, -*Ph*), 4.80 (s, 8H, PhC*H*$_2$), 3.52 (s, 8H, S_2CNCH_2), 2.57-2.30 (m, 24H, NC*H*$_2$), 1.81 (s, 8H, NCH_2CH_2)	208.3 (-*NCS*$_2$), 134.3, 132.8, 129.6, 129.5, 129.1, 128.6, 128.6, 54.9, 53.3, 52.9, 51.5, 51.1, 46.9, 24.1
18	7.36-7.29 (m, 16H, *Ph*), 5.13 (s, 8H, PhC*H*$_2$), 3.81 (s, 8H, S_2CNCH_2), 2.64-2.37 (m, 24H, NC*H*$_2$), 1.81-1.96 (m, 8H, NCH_2CH_2)	205.3 (-*NCS*$_2$), 133.9, 133.6, 129.2, 129.0, 128.6, 57.2, 55.2, 53.0, 52.2, 23.8

5.3 Result and Discussion

5.3.1 Synthesis and Characterization

Secondary diamines viz. *N,N'*-bis{3-(*p*-methoxybenzylamino)propyl}piperazine (**H_2L^5**) and *N,N'*-bis{3-(p-chlorobenzylamino)propyl}piperazine (**H_2L^6**) holding *N,N'*-bispropylpiperazine linkers have been synthesized by following the modified literature procedure[25] as we have discussed in chapter 2, characterized prior to use in the synthesis a new series of metallomacrocyclic dithiocarbamate complexes $[M(II)_2$-μ^2-bis-{(κ^2*S,S*-$S_2CN(R)C_3H_6)_2$piperazine}] wherein R = *p*-methoxy benzyl, M = Ni(II) **13**, Cu(II) **14**, Zn(II) **15**; R = *p*-chlorobenzyl, M = Ni(II) **16**, Cu(II) **17**, Zn(II) **18**, holding bispropyl piperazine linkers (Scheme 1). The one-pot reaction protocol used in the synthesis of these sulphur rich metallomacrocycles has several distinctive advantages as it involves several chemical operations simultaneously in a single vessel, it shortens the workup and ultimately save valued resources.

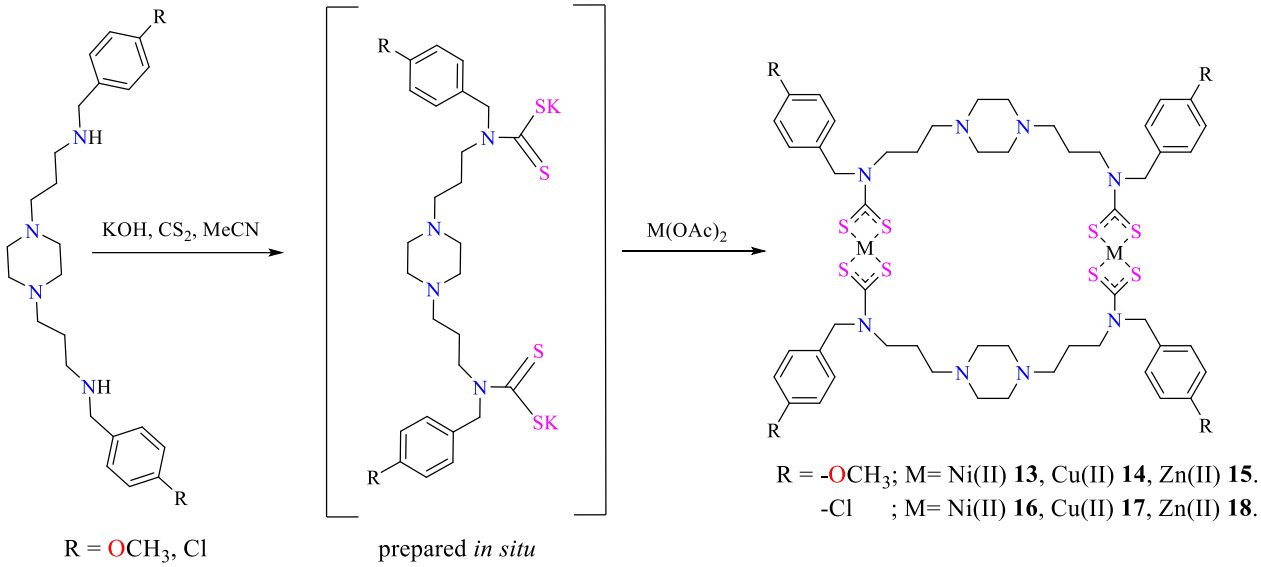

Scheme 1. One-pot multi-component synthetic protocol used for binuclear $Ni^{II}/Cu^{II}/Zn^{II}$ dithiocarbamate metallomacrocyclic compounds holding bispropyl piperazine linkers.

The green coloured Ni(II)-dithiocarbamate compounds (**13, 16**), brown coloured Cu(II)-dithiocarbamate compounds (**14, 17**), and pale yellow coloured Zn(II)-dithiocarbamate compounds (**15, 18**) showed good solubility in polar organic solvents such as DMSO/ DMF. The products were appeared to be air stable in the solid and in the solution state over a period of days.

The compounds were characterized by microanalysis, HRMS (High resolution mass spectrometry), thermogravimetric analysis and relevant spectroscopic techniques. As shown

in table 1 and table 2, the microanalysis and spectroscopic data were sufficient to unequivocally assign the structure of metallomacrocyclic dithiocarbamate complexes **13-18** which were further corroborated by DFT study. The mass analysis was carried out by electrospray ionization (ESI) mode with set parameters, such as gas temperature: 250 °C; drying gas flow: 12 $Lmin^{-1}$; nebulizer pressure: 35 psig; sheath gas flow: 11 $Lmin^{-1}$, sheath gas temperature: 300 °C. The scan source parameters were maintained at capillary voltage: 3.5KV; nozzle voltage: 1.0KV, fragmentor voltage: 175 V; skimmer voltage: 65 V. Mass spectrometric data was processed using MassHunter™ B.08.00 software and the results are presented in Table 3. HRMS spectra of compounds **13**, **15**, **16** and **17** (Annexure 1-4) gave high resolution mass peak for **13** ($C_{56}H_{76}N_8O_4S_8Ni_2$) 1297.2520 $[M+H]^+$, **15** ($C_{56}H_{76}N_8O_4S_8Zn_2$) 1309.2419 $[M+H]^+$, **16** ($C_{52}H_{64}Cl_4N_8S_8Ni_2$) 1313.0708 $[M+H]^+$ and **17** ($C_{52}H_{64}Cl_4N_8S_8Cu_2$) 1322.9199 $[M+H]^+$ with a mass error of 1.16 , 0.61, 11.81 and 93.65 ppm respectively.

Table 3. HRMS data for the compounds under investigation.

Complex	Molecular Formula	Molecular Mass (M.W.)	Calc. mass	Obs. mass	Error(ppm)
13	$C_{56}H_{76}N_8O_4S_8Ni_2$	1296.2462	1297.2535 $[M+H]^+$	1297.2520 $[M+H]^+$	1.16
15	$C_{56}H_{76}N_8O_4S_8Zn_2$	1308.2338	1309.2411 $[M+H]^+$	1309.2419 $[M+H]^+$	0.61
16	$C_{52}H_{64}Cl_4N_8S_8Ni_2$	1312.0481	1313.0553 $[M+H]^+$	1313.0708 $[M+H]^+$	11.81
17	$C_{52}H_{64}Cl_4N_8S_8Cu_2$	1322.0366	1323.0438 $[M+H]^+$	1322.9199 $[M+H]^+$	93.65

All the compounds displayed characteristic IR bands due to ν(C=C), ν(C-N), ν(C-C) and ν(CS_2) in the expected IR regions. The presence of ν(N-H) bands is observed in chapter 2 which is noted being disappeared after the formation of complexes and advent of a new single sharp medium intensity band in 908-985 cm^{-1} range due to $\nu_{assy}(CS_2)$ stretching vibrations in the IR spectra of ensuing metallomacrocyclic compounds **13-18** gave primary indication of bidentate coordination of dithiocarbamate lignads. Besides, the ν(M-S) bands which depends on the metal ion and the auxiliary ligands, appears as medium to weak intensity bands in 533-482 cm^{-1} range.[24c, 25] The IR data is well supported by corresponding NMR spectral study. The presence of benzylic, methoxy, piperazine and diverse methylene groups in the molecules are conformed by ^1H and ^{13}C NMR data as shown in table 2.

Notably, the downfield shifting of *N*-methylene signals by >1 ppm, compared to their positions in free diamines, further supports the formation metallomacrocyclic compounds **13-18** as these signals are most sensitive to any kind of chemical change at amino group. The binuclear metallomacrocyclic dithiocarbamate macrocyclic compounds display a very downfield ^{13}C NMR signal in δ 208.3-204.3 ppm range, characteristic of coordinated dithiocarbamate (-$N^{13}CS_2$) moiety.

5.3.2 UV-Visible absorption and fluorescence spectral study

The electronic absorption spectrum of metallomacrocyclic dithiocarbamate complexes **13-18** was recorded in 10^{-5} M DMSO solution at room temperature (Figure 1, Table 4) and the UV-visible absorption spectral study revealed that Ni(II)-dithiocarbamate complexes **13, 16** and Cu(II)-dithiocarbamate complexes **14, 17** primarily absorbs at ~270 nm, ~320 nm and ~ 400 nm, attributable to π→π* (phenyl) and n→π* (amine) and charge transfer transitions, respectively. Notably, Cu(II) complexes **14, 17** displayed d-d bands at ~620 nm while Zn(II) complexes **15** and **18** exhibited featureless absorption spectra presenting a broad absorption at ~270 nm due to intra-ligand π→π* transitions. Magnetic moment along with UV-visible absorption bands suggest square planar/distorted square planar environment around nickel(II)/ copper(II) and tetrahedral/distorted tetrahedral environment around zinc(II) centres in their respective complexes.

Evidently, Ni(II)/Zn(II)-dithiocarbamate complexes gave intense fluorescence emission in the visible region upon excitation at lower wavelengths whereas relatively poor emission bands are expectedly observed for Cu(II)-dithiocarbamate complexes **14** and **17**.

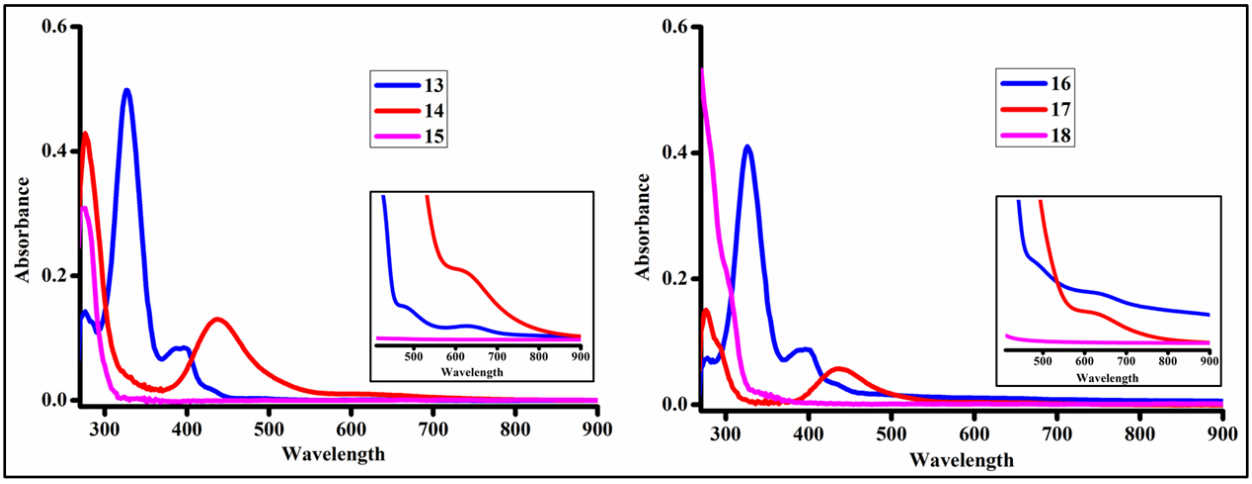

Figure 1. UV-visible absorption spectra of metallomacrocyclic dithiocarbamate complexes **13-18** in 10^{-5} M DMSO solution at room temperature.

Table 4. UV-visible absorption, magnetic moment and fluorescence data for metallomacrocyclic dithiocarbamate complexes **13-18**.

Entry	UV-Visible data (10^{-5} M DMSO) λ_{max} nm (ε, L mol^{-1} cm^{-1})	Magnetic moment μ_{eff} (BM)	Fluorescence data (10^{-5} M DMSO)	
			λ_{em} nm (Intensity)	λ_{ex} (nm)
13	275 (13791) π→π*, 330 (49682) n→π*, 392 (8809) CT	0	365 (1191), 407 (578), 440 (471)	328
14	276 (42571) π→π*, 321 (4440) n→π*, 438 (12734) CT, 619(1007) d-d	1.84	507 (285)	439
15	274 (31434) π→π*	0	294(1893), 333(2176)	268
16	276 (7432) π→π*, 326 (40356) n→π*, 401 (8962) CT, 674 (940) d-d	0	-	-
17	277 (15264) π→π*, 294 (15707) n→π*, 437 (6002) CT, 627 (408) d-d	1.89	-	-
18	268 (53243) π→π*	0	-	-

5.3.3 Thermogravimetric Analysis

The binuclear metallomacrocyclic dithiocarbamate complexes **13-18** are thermally stable upto ~200 ºC and their diversified rate of degradation can be clearly visualized from their DTG curves, recorded under similar heating rate of 10 ºC min^{-1} under nitrogen atmosphere. (Figure 2) Notably, the TG curves of compounds **14**, **15** and **17** gave the mass loss of 81.0, 85.0 and 81.4 % respectively, and thus their stable residual mass obtained at 700 ºC corresponds to corresponding metal sulphides. (Table 5) The results of thermogravimetric study clearly revealed that copper(II) complexes **14**, **17** and a zinc(II) complex **15** have the potentials to be utilized as single source precursors for the synthesis of high quality nanoscale binary, ternary and quaternary metal sulphides which are indeed emerging as a new class of resources for energy conversion and/or storage applications due to their low cost and high electrochemical activity.

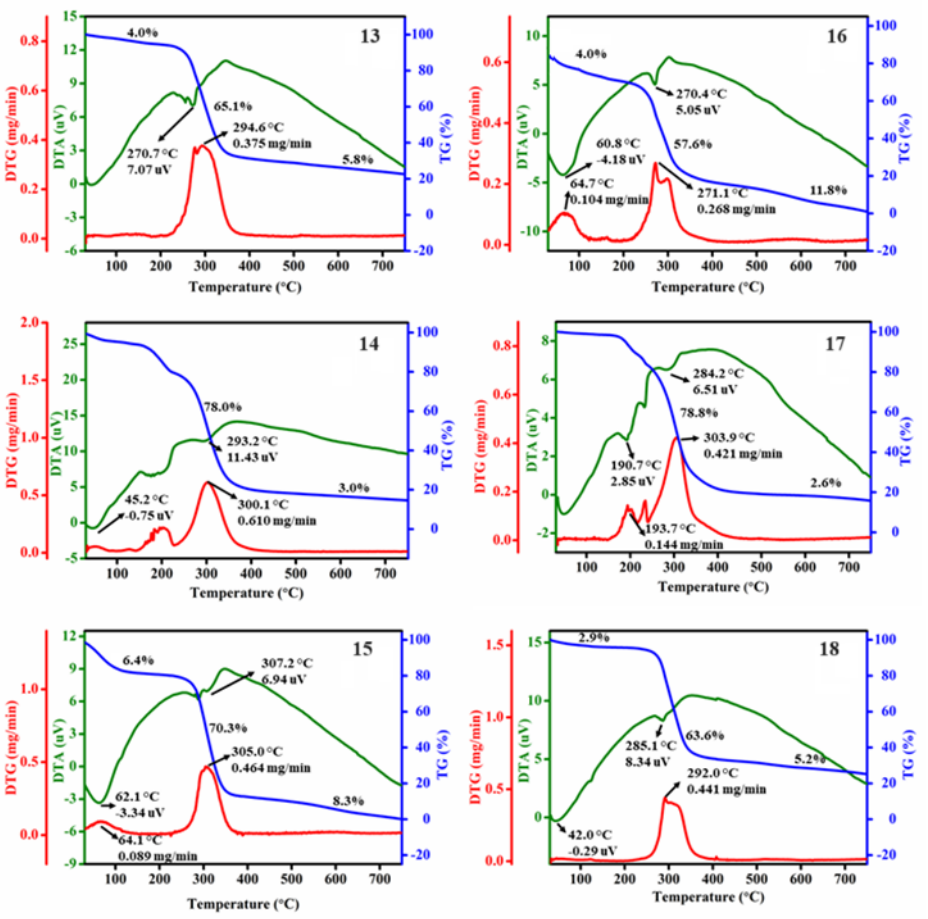

Figure 2. TG/DTA curves for metallomacrocyclic dithiocarbamate complexes **13-18**.

Table 5. Thermogravimetric analysis of metallomacrocyclic dithiocarbamate complexes **13-18.**

Entry	T (°C) in DTA	T (°C) in TGA	Mass loss obs. (%) in TG	Residue wt. obs. (Calcd.) (%)	Expected product of decomposition
13	270.7	200-400	69.1	25.1	$NiSO_4$ + plus char
		400-700	5.8	(23.8)	
14	293.2	150-400	78.0	19.0	CuS + plus char
		400-700	3.0	(14.6)	
15	307.2	100-400	86.7	15.0	ZnS
		400-700	8.3	(14.9)	
16	270.4	70-400	61.6	26.6	$NiSO_4$ + plus char
		400-700	11.8	(23.5)	
17	284.2	200-400	78.8	18.6	CuS + plus char
		400-700	2.6	(14.4)	
18	285.1	100-400	66.5	28.3	$ZnSO_4$ + plus char
		400-700	5.2	(24.3)	

5.3.4 Density functional theory calculations

Density functional theory level calculations and full geometry optimizations were carried out for binuclear dithiocarbamate complexes **13-18** using B3LYP/LanL2DZ basis sets and the

molecular orbitals were generated by GaussView 16.0 program.[26] The optimized structures for the minimum energy conformation of complexes **13-18** are presented in Figure 3.

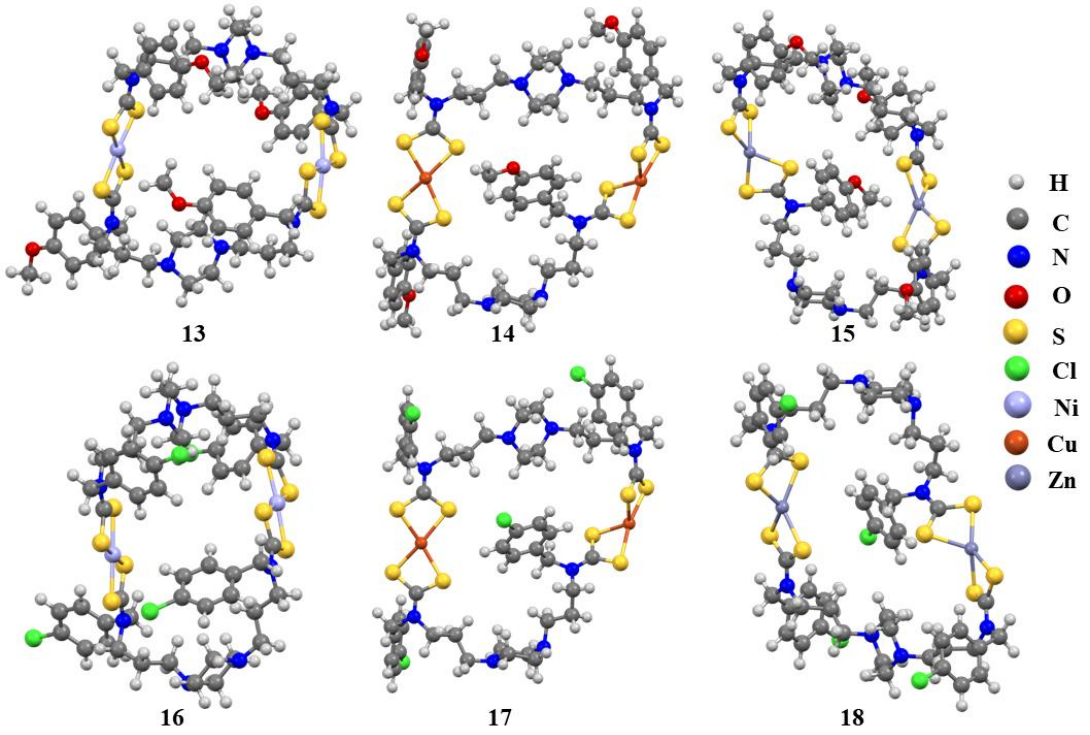

Figure 3. An optimized geometry for the minimum energy conformation of complexes **13-18** at B3LYP/LanL2DZ level.

The structural parameters (selected bond lengths and bond angles) of binuclear metallomacrocyclic dithiocarbamate complexes **13-18** are found to be consistent with the similar parameters deduced experimentally for analogous compounds[24b,27] by means of single crystal XRD. A closer inspection of the structural parameters shows that the calculated N-C and C-S bond distances (Å) in **13-18** matches well with the similar distances obtained experimentally for closely related compounds,[24b, 27] however, calculated M-S bond distances are slightly overestimated, compared to the experimental data. Similarly, the calculated S-M-S (chelate) bond angle (°) in **13-18** are in good agreement with the similar values obtained from X-ray analysis and validates the theoretical calculations performed on **13-18**. In comparison with the Cu(II)-dithiocarbamate compounds (**14, 17**), Ni(II)-dithiocarbamate compounds (**13, 16**) showed less distinct Ni–S distances from each other, 2.265–2.292 Å and indicates the coordination mode of the dithiocarbamate moieties closer to symmetrical isobidentate. Moreover, a slight deviation in the chelate ring planes (~5°) from coplanarity indicates the geometry around both the nickel(II) centers in **13** and **16** are closer to square planar. In Zn(II)-dithiocarbamate compounds (**15, 18**), S-M-S bond angles deviates

significantly from each other (109.15-140.95°) suggesting distortion of geometry around both the zinc(II) centers from tetrahedron. The calculated structures gave C–N bond distances of the dithiocarbamate groups in the range 1.337–1.344 Å and indicate the presence of sp^2 hybridized nitrogen atoms due to π-electron delocalization between the nitrogen and sulphur. The sizes of the macrocyclic cavities in the molecular structures of binuclear metallomacrocyclic dithiocarbamate complexes **13-18** can be best visualized from trans-annular M-M, trans piperazine N-N and trans dithiocarbamate N-N distances (Table 6).

Table 6. Comparison of selected geometrical parameters for macrocyclic dithiocarbamate complexes **13-18** obtained from theoretical study with similar experimental parameters retrieved from the literature.

Compound	**Bond length (Å)**						**Bond angles (°)**	
	N-C	C-S	M-S	Trans-annular M-M	N-N (Trans piperazine)	N-N (trans NCS_2)	S-M-S (chelate)	S-M-S
13	1.337 to 1.340	1.731 to 1.738	2.272 to 2.284	10.559	10.340	11.037	78.26 to 78.35	171.88 to 179.44
16	1.338 to 1.339	1.731 to 1.737	2.265 to 2.292	8.485	13.045	9.221	78.30 to 78.34	176.54 to 178.47
Ni^{II}-dtc[27a]	1.281 to 1.508	1.691 to 1.744	2.164 to 2.225	-	-	-	78.99 to 79.87	100.31 to 177.14
14	1.339 to 1.343	1.735 to 1.746	2.367 to 2.430	11.820	12.316	15.213	75.26 to 75.57	109.64 to 160.77
17	1.340 to 1.344	1.733 to 1.746	2.363 to 2.437	11.699	12.404	15.255	75.19 to 75.54	109.64 to 160.77
Cu^{II}-dtc[24b]	1.318 to 1.328	1.719 to 1.727	2.288 to 2.301	-	-	-	77.59	101.72 to 103.48
15	1.342	1.743 to 1.756	2.421 to 2.444	10.199	12.482	14.830	75.58 to 76.29	122.36 to 131.08
18	1.342 to 1.343	1.741 to 1.756	2.430 to 2.460	10.193	12.888	14.788	75.29 to 75.87	123.69 to 129.58
Zn^{II}-dtc[27b]	1.333 to 1.363	1.717 to 1.782	2.32 to 2.44	-	-	-	79.5 to 81.2	126.53 to 136.00

The macrocyclic cavities in these compounds could not be affected significantly due to presence of distinct *N*-substituents at the peripheral positions of macrocyclic framework. Interestingly, one of the peripheral *N*-benzylic substituents positioned towards inward direction of the macrocyclic cavity, acting as a base of the cavity. A comparative view of the molecular structures corresponding to the calculated lowest-energy structures of the binuclear dithiocarbamate complexes **13-18** is displayed in Figure 4.

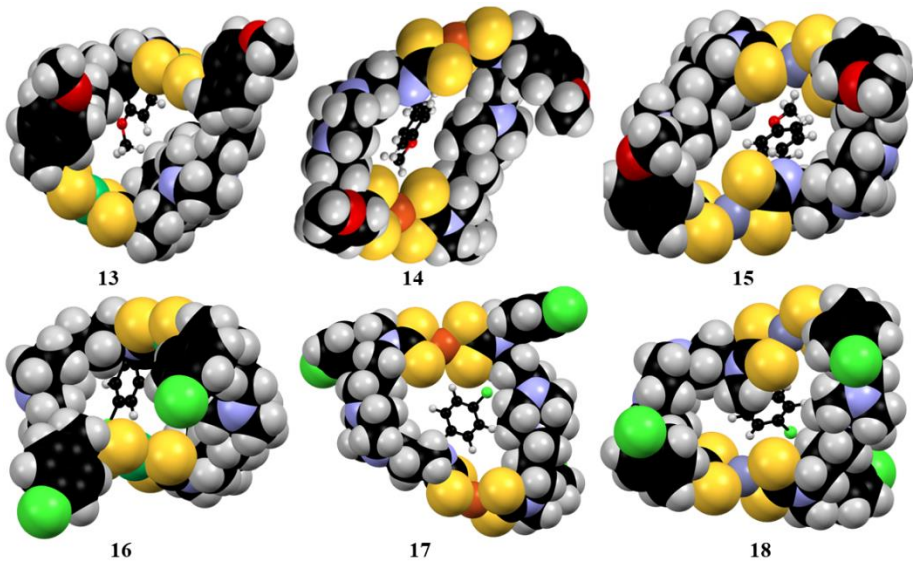

Figure 4. Spacefill model presenting the orientation of one of the peripheral *N*-benzylic groups towards inward direction of the macrocyclic cavity in **13-18**.

The molecular electrostatic potential (MESP) maps of **13–18** offer valuable information by clearly demonstrating that the areas with high electron density are mostly localized around the dithiocarbamate chelate rings. (Figure 5)

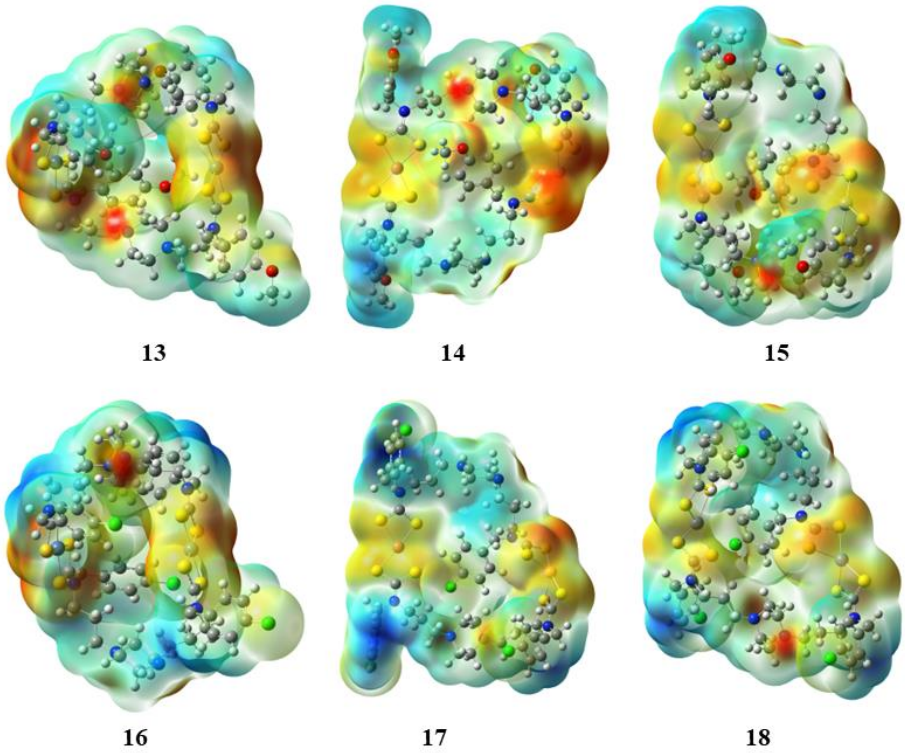

Figure 5. Representations of electron density from total SCF density (Isovalue= 0.0004; mapped with ESP)

The analysis of highest occupied molecular orbitals (HOMO) and lowest occupied molecular orbitals (LUMO) in binuclear metallomacrocyclic dithiocarbamate complexes **13-**

18 indicates that the HOMO of **13-18** is exclusively delocalized on the one of piperazine ring, whereas, The LUMO in **13-18** is delocalized on one of the coordinated dithiocarbamate moiety (Figure 6). The calculated HOMO-LUMO energy gaps for binuclear metallomacrocyclic dithiocarbamate complexes **13-18** are given in Table 7 is illustrated in Figure 6. Notably, the HOMO-LUMO band gaps calculated for both the Cu(II)-dithiocarbamate (**14, 17**) falls in the range of 1.19-1.33 eV, indicating their semiconducting nature.[28]

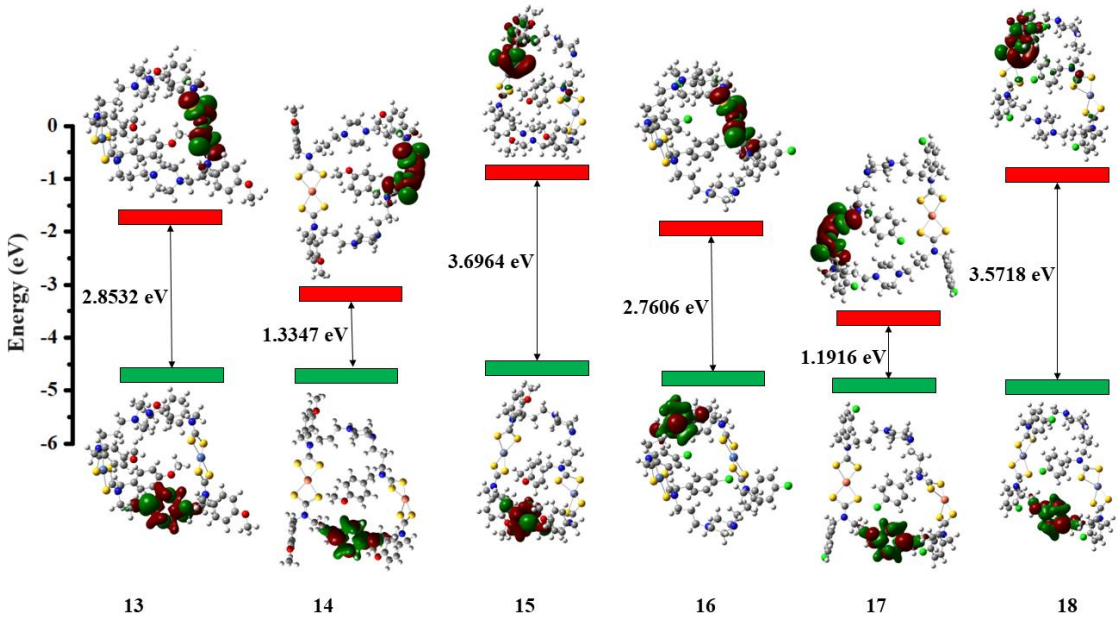

Figure 6. Comparison of the frontier molecular orbitals derived from DFT calculation at the B3LYP/ LanL2DZ level for metallomacrocyclic dithiocarbamate complexes **13-18**.

The energy of geometry optimization and HOMO-LUMO band gaps for binuclear metallomacrocyclic dithiocarbamate complexes **13-18** are tabulated in Table 7.

Table 7. Summary of Computational study performed on complexes **13-18.**

Entry	Energy (Hartree)	HOMO (eV)	LUMO (eV)	Band Gap (eV)
13	-6442.825820	-4.7073	-1.8541	2.8532
14	-6496.466663	-4.7040	-3.3693	1.3347
15	-6235.447261	-4.6447	-0.9483	3.6964
16	-7823.114670	-4.8107	-2.0501	2.7606
17	-7876.747121	-4.8929	-3.7013	1.1916
18	-7615.676708	-4.8472	-1.2754	3.5718

5.4 Heavy metal ions sensing study

The binuclear metallomacrocyclic dithiocarbamate compounds **13-18** possessing Lewis basic coordinating groups along with a number of features (vide supra) were anticipated to be proven as promising small molecule probe to sense/ bind environmentally hazardous heavy metal ions such as Pb(II), Cd(II) and Hg(II). Identification of new probe that is cost effective, rapid, facile and applicable to the environmental settings is an important goal of sensing societies due to current concern over heavy metal ions in the environment and its toxic effects on human health. The new probe becomes more important in case of Pb(II), Cd(II) and Hg(II) ions as these ions have no optical sign due to their closed-shell d^{10} configuration. Optical detection through changes in UV–visible or fluorescence spectra resulted from perturbations due to heavy metal ions would be highly appropriate for monitoring these heavy metal ions in environmental frameworks. Such small-molecule probe suitable for optical read-outs of heavy metal ions upon complexation can suitably be designed into analysis tools, optical devices or profitable indicators, helping rapid detections of Pb(II), Cd(II) and Hg(II) ions in the laboratory.

Our experimental outcomes could not be supported well due to lack of literature support on the sensing study of heavy metal ions involving inorganic dithiocarbamate macrocyclic structures by using either UV-visible or fluorescence spectral studies. We have selected macrocycles **13** and **14** for detailed sensing study of heavy metal ions because *N*-benzylic substituents are not affecting the cavity size of 34-membered metallomacrocyclic dithiocarbamate compounds **13-18** significantly. Evidently, macrocycles **13** and **14** exhibited absorption maxima at 331 nm and 276 nm in their UV/vis spectrum, respectively. Notably, Ni(II)-dithiocarbamate complex **13** upon binding with Pb(II) induced a significant blue-shift *ca* 6 nm with increase in the molar extinction coefficient by 2575 L mol^{-1} cm^{-1}. The interaction of **13** with Cd(II) causing a measurable increase in the molar extinction coefficient by 657 L mol^{-1} cm^{-1} without significant shifting in the absorption band. Contrarily, the interaction of Cu(II)-dithiocarbamate complex **14** with Cd(II) causing a measurable decrease in the molar extinction coefficient by 1196 L mol^{-1} cm^{-1} with a significant red-shifting in the absorption band *ca* 5 nm as demonstrated by Figure 7.

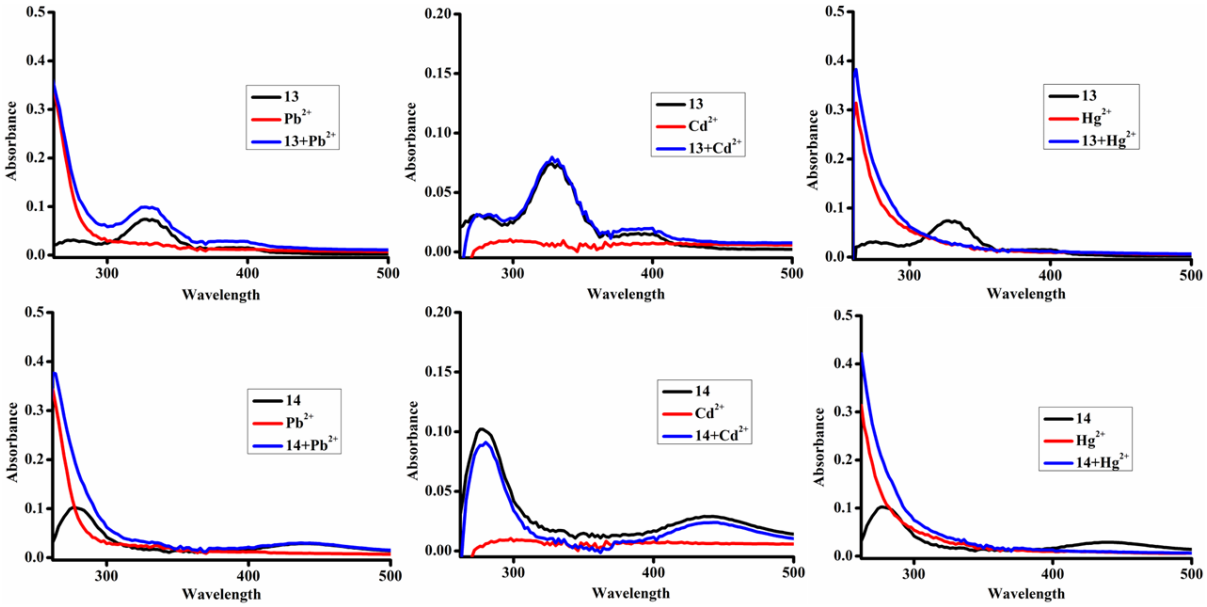

Figure 7. Metallomacrocycles **13-14** (c, 10 μM) as a sensing probe for Pb(II), Cd(II) and Hg(II) ions (c, 0.4 mM) in DMSO by using UV-visible spectroscopy.

Interestingly, the UV/vis absorption maxima disappears upon addition of Pb(II) ions (in case of **14** only) and softer Hg(II) ions (both in case **13** and **14**).

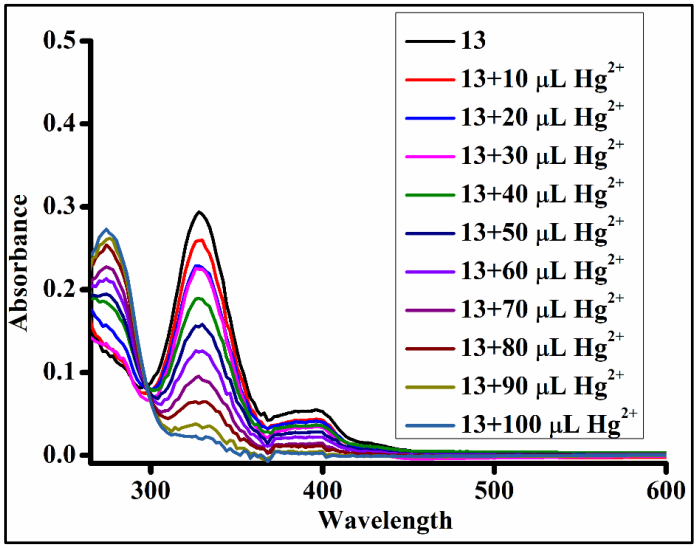

Figure 8. Absorption titration spectra of probe **13** (c, 10 μM) in the presence of various equivalents of Hg(II) ions (0.0−1.0 equiv; 0.2 mM) in DMSO.

The UV-visible titration study (Figure 8) clearly revealed that the peak at ~330 nm within the UV-vis spectrum of Ni(II)-dithiocarbamate complex **13** decreased gradually upon the addition of Hg(II), whereas the absorbance intensity at ~274 nm gradually increased with one isobestic point[12] determined at 298 nm, indicating that a new product is generated upon binding to Hg(II).

Moreover, a careful literature survey suggest that 3d-metal complexes are scarcely been developed as fluorescent probes for cation sensing study.[12b, 29] Thus, it was highly desirable to explore the ability of Cu(II)/ Zn-dithiocarbamate complexes (**14** or **15)** as a fluorescence chemosensing probe for the detection of heavy metal ions.

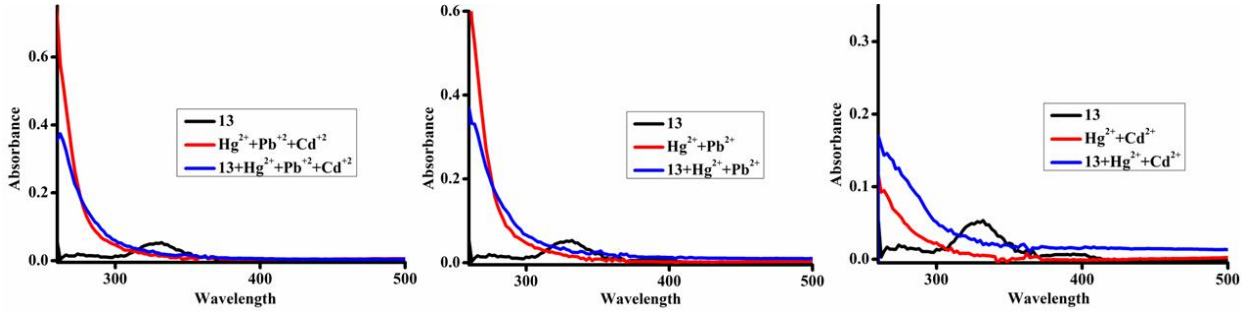

Figure 9. Absorption spectra of **1** (c, 10 μM) in the presence of Hg(II), Pb(II) and Cd(II) ions as interfearing (c, 0.4 mM) in DMSO.

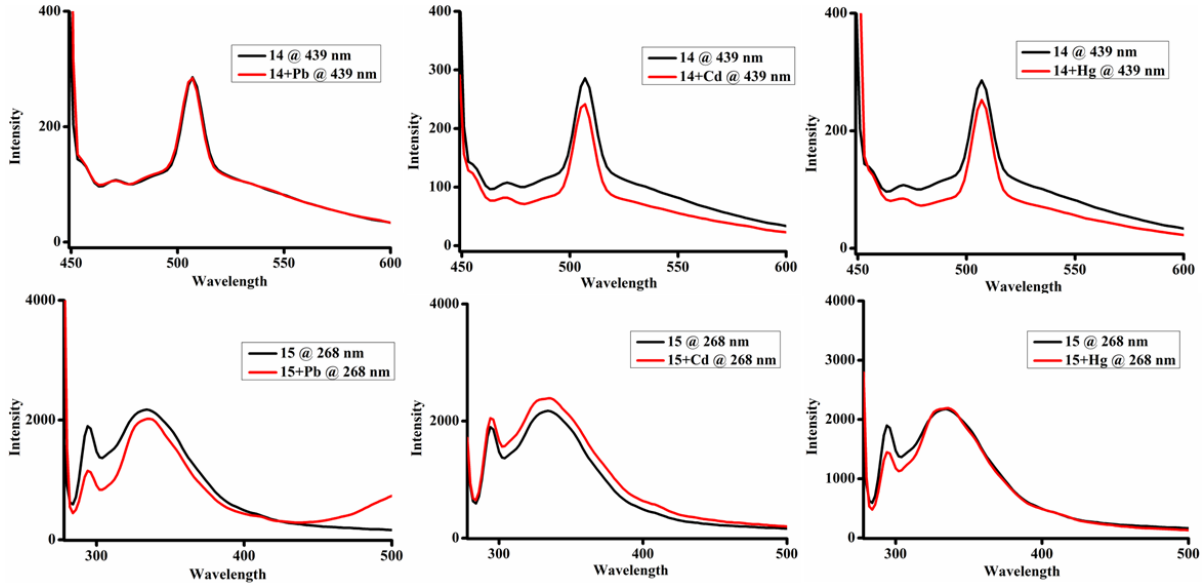

Figure 10. Fluorescence spectra of **14-15** (c, 10 μM) in the presence of Hg(II), Pb(II) and Cd(II) ions (c, 0.4 mM) in DMSO.

Evidently, the addition of nearly one equivalent of Pb(II), Cd(II) or Hg(II) heavy metal ions to a solution of *N,N'*-bis(3-dithiocarbamatopropyl) piperazine bridged fluorescent Cu(II)/ Zn-based probes **14-15** resulted into substantial fluorescence quenching (Figure 10), apparently due Pb(II)/Cd(II)-induced perturbation of a chromophore.[1] Earlier report suggests that addition of one equiv. of Zn(II) to the nonfluorescent phenylene-bridged bis(pyrrol-2-ylmethyleneamine) ligand in MeCN afford access to a fluorescent Zn(II) complex which upon interaction with Hg(II) ions led the formation of the nonemissive Hg(II) complex.[30] Contrarily, the addition of Pb(II), Cd(II) or Hg(II) metal ions to a solution of Ni(II)-based probe **13** resulted into considerable increase in the fluorescence intensity which can be clearly

visualized from the fluorescence titration study (Figure 11). Evidently, concomitant increase in the fluorescence intensity by ~2 folds of **13** was observed on addition of 10 equivalent solution of Pb(II), Cd(II).

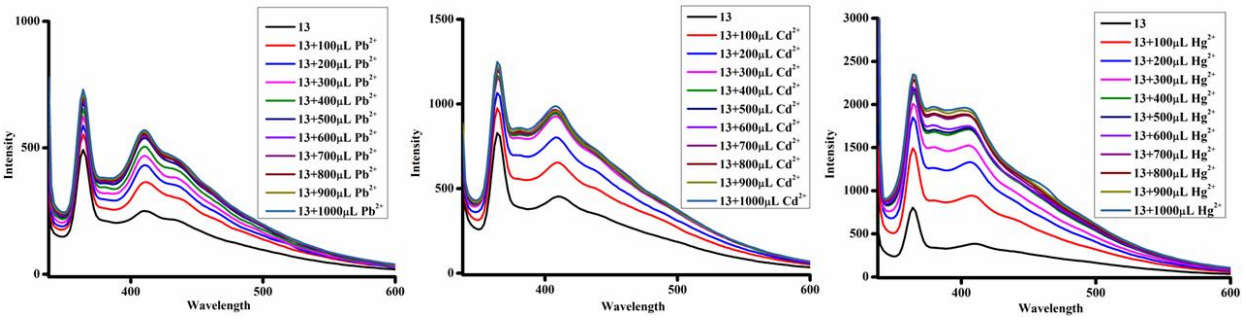

(a) **(b)** **(c)**

Figure 11. Fluorescence titration spectra of probe **13** (c, 10 μM) in the presence of (a) Pb(II) (0.0−10.0 equiv; c, 0.2 mM), (b) Cd(II) (0.0−10.0 equiv; c, 0.2 mM) and (c) Hg(II) (0.0−10.0 equiv; c, 0.2 mM) in DMSO under a UV lamp irradiated at 328 nm.

5.5 Conclusions

This study allows us to conclude that a new series of *N,N'*-bis(3-dithiocarbamatopropyl) piperazine bridged metallomacrocyclic complexes [M(II)$_2$-μ^2-bis-{(κ^2*S,S*-$S_2CN(R)C_3H_6)_2$piperazine}] (R = *p*-methoxybenzyl, M = Ni(II) **13**, Cu(II) **14**, Zn(II) **15**; R = *p*-chlorobenzyl, M = Ni(II) **16**, Cu(II) **17**, Zn(II) **18**) can be conveniently synthesized by using a single pot-multi component reaction protocol. The phase purity and formulation of these were thoroughly verified by microanalysis, relevant spectroscopies, validated by density functional theory calculations. Interestingly, critical analysis of TG curves indicates the potentials of compounds **14**, **15** and **17** to form high purity metal sulphides (MS) nanoparticle that can form a new class of resources for energy conversion and/or storage applications whereas the analysis of HOMO-LUMO band gaps indicates the semiconducting nature Cu(II)-dithiocarbamate **14** and **17**. It is worth noting that the use of soft sulphur donor atoms in the chelating unit of metallomacrocycles **13-18** evidently increase their affinity and selectivity for Hg(II) ions over Pb(II) and Cd(II). A comprehensive literature survey reveals that dithiocarbamate complex based UV-visible/ fluorescent chemosensors have not yet been described for heavy metal ions except for Li^+, Na^+, K^+, Cs^+, neutral organic or anionic guest species such as halides, $H_2PO_4^-$, CH_3COO^-, and $C_6H_5COO^-$. Thus, our explorations on the use of sulphur rich metallomacrocyclic compounds as small-molecule probe for optical read-outs of environmentally hazardous heavy metal ions, preferably Hg(II) ions over Pb(II) and

Cd(II) add merit to this work. The results further suggest that such transition metal dithiocarbamate based molecular probe can be suitably designed as an analysis tools, optical devices or profitable indicators to assist rapid detections of hazardous metal ions in the laboratory.

5.6 References

[1] Carter, K. P.; Young, A. M.; Palmer, A. E. *Chem. Rev*. **2014**, *114*, 4564.

[2] Martinez-Finley, E. J.; Chakraborty, S.; Fretham, S. J. B.; Aschner, M. *Metallomics.*, **2012**, *4*, 593.

[3] (a) Thévenod, F. *Toxicol. Appl. Pharmacol*. **2009**, *238***,** 221; (b) Bridges, C. C.; Zalups, R. K. *Toxicol. Appl. Pharmacol.* **2005**, *204***,** 274.

[4] Zhou, X.; Li, P.; Shi, Z.; Tang, X.; Chen, C.; Liu, W. *Inorg. Chem.* **2012**, *51***,** 9226.

[5] (a) Kim, H. N.; Ren, W. X.; Kim, J. S.; Yoon, J. *Chem. Soc. Rev.* **2012**, *41*, 3210; (b) Nolan, E. M.; Lippard, S. J. *Chem. Rev.* **2008**, *108*, 3443.

[6] Unterreitmaier, E.; Schuster, M. *Anal. Chim. Acta.* **1995**, *309*, 339.

[7] Medina, I.; Rubí, E.; Mejuto, M. C.; Cela, R. *Talanta.* **1993**, *40*, 1631.

[8] Krawczyk, T. K.; Moszczyn´ska, M.; Trojanowicz, M. *Biosens. Bioelectron.* **2000**, *15*, 681.

[9] (a) Zhao, Q.; Cao, T.; Li, F.; Li, X.; Jing, H.; Yi, T.; Huang, C. *Organometallics.* **2007**, *26*, 2077; (b) Caballero, A.; Lloveras, V.; Curiel, D.; Tárraga, A.; Espinosa, A.; García, R.; Vidal-Gancedo, J.; Rovira, C.; Wurst, K.; Molina, P.; Veciana, J. *Inorg. Chem.* **2007**, *46*, 825; (c) Muthukumar, C.; Kesarkar, S. D.; Srivastava, D. N. *J. Electroanal. Chem.* **2007**, *602*, 172.

[10] (a) Biological Inorganic Chemistry, 1st ed.; Bertini, I.; Gray, H. B.; Stiefel, E. I.; Valentine, J. S.; Eds.; University Science Books: Sausalito, CA, 2007; (b) Paw, R.; Hazarika, M.; Boruah, P. K.; Kalita, A. J.; Guha, A. K.; Das, M. R.; Tamuly, C. *RSC Adv.* **2021**, *11*, 14700.

[11] McRae, R.; Bagchi, P.; Sumalekshmy, S.; Fahrni, C. *J. Chem. Rev.* **2009**, *109*, 4780.

[12] (a) Pandey, R.; Gupta, R. K.; Shahid, M.; Maiti, B.; Misra, A.; Pandey, D. S. *Inorg. Chem.* **2012**, *51*, 298; (b) Pandey, R.; Kumar, A.; Xu, Q.; Pandey, D. S. *Dalton Trans.* **2020**,*49*, 542.

[13] (a) Yoon, S.; Albers, A. E.; Wong, A. P.; Chang, C. J. *J. Am. Chem. Soc.* **2005**, *127*, 16030; (b) Lin, W.; Cao, X.; Ding, Y.; Yuan, L.; Yu, Q. *Org. Biomol. Chem.* **2010**, *8*, 3618; (c) Lin, W.; Cao, X.; Ding, Y.; Yuan, L.; Long, L. *Chem. Commun.* **2010**, *46*, 3529.

[14] Wang, H.; Li, Y.; Xu, S.; Li, Y.; Zhou, C.; Fei, X.; Sun, L.; Zhang, C.; Li, Y.; Yang, Q.; Xu, X. *Org. Biomol. Chem.* **2011**, *9*, 2850.

[15] Hatai, J.; Pal, S.; Jose, G. P.; Bandyopadhyay, S. *Inorg. Chem.* **2012**, *51*, 10129.

[16] (a) Costero, A. M.; Andreu, R.; Monrabal, E.; Martínez-Máñez, R.; Sancenón, F.; Soto, J. *J. Chem. Soc. Dalton Trans.* **2002**, 1769; (b) Zhu, X.-J.; Fu, S.-T.; Wong, W.-K.; Guo, J.-P.; Wong, W.-Y. *Angew.Chem. Int. Ed.* **2006**, *45*, 3150.

[17] (a) Métivier, R.; Leray, I.; Valeur, B. *Chem. Eur. J.* **2004**, *10*, 4480; (b) Chen, Q.-Y.; Chen, C.-F. *Tetrahedron Lett.* 2005, *46*, 165; (c) Kim, J. H.; Hwang, A.-R.; Chang, S.-K. *Tetrahedron Lett.* **2004**, *45*, 7557.

[18] Kim, S. H.; Song, K. C.; Ahn, S.; Kang Y. S.; Chang, S.-K. *Tetrahedron Lett.* **2006**, *47*, 497.

[19] (a) Moon, S.-Y.; Youn, N. J.; Park, S. M.; Chang, S.-K. *J. Org. Chem.* **2005**, *70*, 2394; (b) Park, S. M.; Kim, M. H.; Choe, J.-I.; No, K. T.; Chang, S.-K. *J. Org. Chem.* **2007**, *72*, 3550.

[20] (a) Wang, L.; Wong, W.-K.; Wu, L.; Li, Z.-Y. *Chem. Lett.* **2005**, *34*, 934; (b) Wang, L.; Zhu, X.-J.; Wong, W.-Y.; Guo, J.-P.; Wong, W.-K.; Li, Z.-Y. *J. Chem. Soc.* Dalton Trans. **2005**, 3235.

[21] (a) Rurack, K.; Resch-Genger, U.; Bricks, J. L.; Spieles, M. *Chem. Commun.* **2000**, 2103; (b) Rurack, K.; Kollmannsberger, M.; Resch-Genger, U.; Daub, J. *J. Am. Chem. Soc.* **2000**, *122*, 968; (c) Kadarkaraisamy, M.; Sykes, A. G. *Polyhedron.* **2007**, *26*, 1323.

[22] (a) Singh, V. K.; Pillai, V.; Patel, S. K.; Buch, L. *ChemistrySelect.* **2019**, *4*, 8689; (b) Pillai, V. Patel, S. K.; Buch, L.; Singh, V. K. *Appl. Organomet. Chem.* **2018**, *32*, e4559; (c) Pillai, V.; Buch, L.; Desai, A.; Singh, V. K. *ChemistrySelect*. **2017**, *2*, 11581; (d) Pillai, V.; Kadu, R.; Buch, L.; Singh, V. K. *ChemistrySelect*. **2017**, *2*, 4382; (e) Kadu, R.; Roy, H.; Singh, V. K. *Appl. Organometal. Chem.* **2015**, *29*, 746.

[23] (a) Lee, S. M.; Tiekink, E. R. T. *Inorganics.* **2021**, *9*, 7; (b) Rojas-León, I.; Alnasr, H.; Jurkschat, K.; Vasquez-Ríos, M. G.; Gómez-Jaimes, G.; Höpfl, H.; Hernández-Ahuactzí, I. F.; Santillan, R. *Organometallics.* **2019**, *38*, 2443; (c) Torres-Huerta, A.; Höpfl, H.; Tlahuext, H.; Hernández-Ahuactzi, I. F.; Sánchez, M.; Reyes-Martínez, R.; Morales-Morales, D. *Eur. J. Inorg. Chem.* **2013**, 61; (d) Torres-Huerta, A.; Cruz-Huerta, J.; Höpfl, H.; Hernández-Vázquez, L. G.; Escalante-García, J.; Jiménez-Sánchez, A.; Santillan, R.; Hernández-Ahuactzi, I. F.; Sánchez, M. *Inorg. Chem.* **2016**, *55*, 23, 12451; (e) Cruz-Huerta, J.; Carillo-Morales, M.; Santacruz-Juárez, E.; Hernández-Ahuactzi, I. F.; Escalante-García, J.; Godoy-Alcantar, C.; Guerrero-Alvarez, J. A.; Höpfl, H.; Morales-Rojas, H.; Sánchez, M. *Inorg.*

Chem. **2008**, *47*, 21, 9874; (f) Selvaganapathi, P.; Thirumaran, S.; Ciattini, S. **2019**, *33*, e5089.

[24] (a) Beer, P. D.; Berry, N. G.; Cowley, A. R.; Hayes, E. J.; Oates, E. C.; Wong, W. W. H. *Chem. Commun.* **2003**, 2408; (b) Cookson, J.; Evans, E. A. L.; Maher, J. P.; Serpell, C. J.; Paul, R. L.; Cowley, A. R.; Drew, M. G. B.; Beer, P. D. *Inorg. Chim. Act.* **2010**, *363*, 1195; (c) Kadu, R.; Pillai, V.; Amrit, V.; Singh, V. K. *RSC Adv.* **2015**, *5*, 106688.

[25] (a) A. Z. E.-Sonbati, *Synth. React. Inorg. Met. -Org. Chem*. **1991**, *21*, 203; (b) K. S. Siddiqi, S. A. A. Lutfullah Nami, Y. Chebude, *J. Braz. Chem. Soc.* **2006**, *17*, 107; (c) F. Bensebaa, Y. Zhou, A. G. Brolo, D. E. Irish, Y. Deslandes, E. Kruus, T. H. Ellis, *Spectrochim. Acta*. **1999**, *55*, 1229.

[26] M. J. Frisch, G. W. Trucks, H. B. Schlegel, G. E. Scuseria, M. A. Robb, J. R. Cheeseman, G. Scalmani, V. Barone, G. A. Petersson, H. Nakatsuji, X. Li, M. Caricato, A. V. Marenich, J. Bloino, B. G. Janesko, R. Gomperts, B. Mennucci, H. P. Hratchian, J. V. Ortiz, A. F. Izmaylov, J. L. Sonnenberg, D. Williams-Young, F. Ding, F. Lipparini, F. Egidi, J. Goings, B. Peng, A. Petrone, T. Henderson, D. Ranasinghe, V. G. Zakrzewski, J. Gao, N. Rega, G. Zheng, W. Liang, M. Hada, M. Ehara, K. Toyota, R. Fukuda, J. Hasegawa, M. Ishida, T. Nakajima, Y. Honda, O. Kitao, H. Nakai, T. Vreven, K. Throssell, J. A. Montgomery, Jr., J. E. Peralta, F. Ogliaro, M. J. Bearpark, J. J. Heyd, E. N. Brothers, K. N. Kudin, V. N. Staroverov, T. A. Keith, R. Kobayashi, J. Normand, K. Raghavachari, A. P. Rendell, J. C. Burant, S. S. Iyengar, J. Tomasi, M. Cossi, J. M. Millam, M. Klene, C. Adamo, R. Cammi, J. W. Ochterski, R. L. Martin, K. Morokuma, O. Farkas, J. B. Foresman, D. J. Fox, Gaussian, Inc., Wallingford CT, **2016**.

[27] (a) P. D. Beer, A. G. Cheetham, M. G. B. Drew, O. Danny Fox, J. Elizabeth Hayes, T. D. Rolls, *Dalton Trans*. **2003**, *4*, 603; (b) S.-W. Lai, M. G. B. Drew, P. D. Beer, *J. Organomet. Chem.* **2001**, *637*, 89.

[28] S. K. Patel, K. Kolte, C. J. Savani, P. Raghavaiah, D. Dave, A. A. Isab, D. Mistry, D. Suthar, V. K. Singh, *Inorg. Chim. Acta.* **2022**, *543*, 121139.

[29] J. Cheng, X. Zhou, H. Xiang, *Analyst*, **2015**, *140*, 7082.

[30] Z. Wu, Q. Chen, S. Xiong, B. Xin, Z. Zhao, L. Jiang, J. S. Ma, *Angew. Chem. Int. Ed.* **2003**, *42*, 3271.

5.7 Annexures

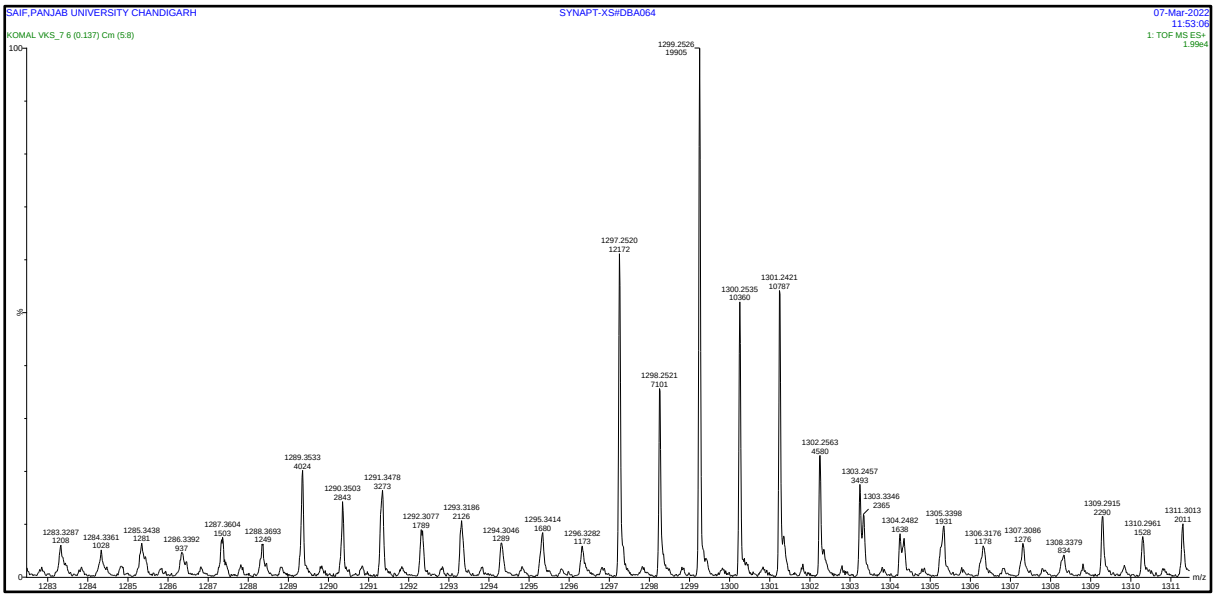

Annexure 1. HRMS spectrum of Complex **13**.

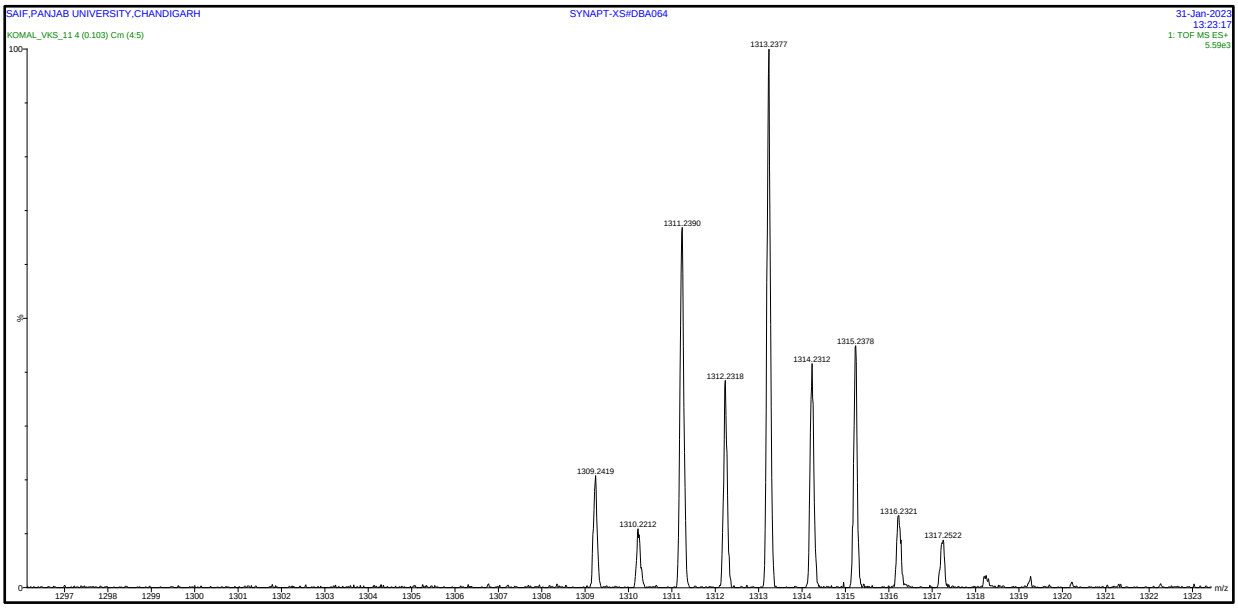

Annexure 2. HRMS spectrum of Complex **15**.

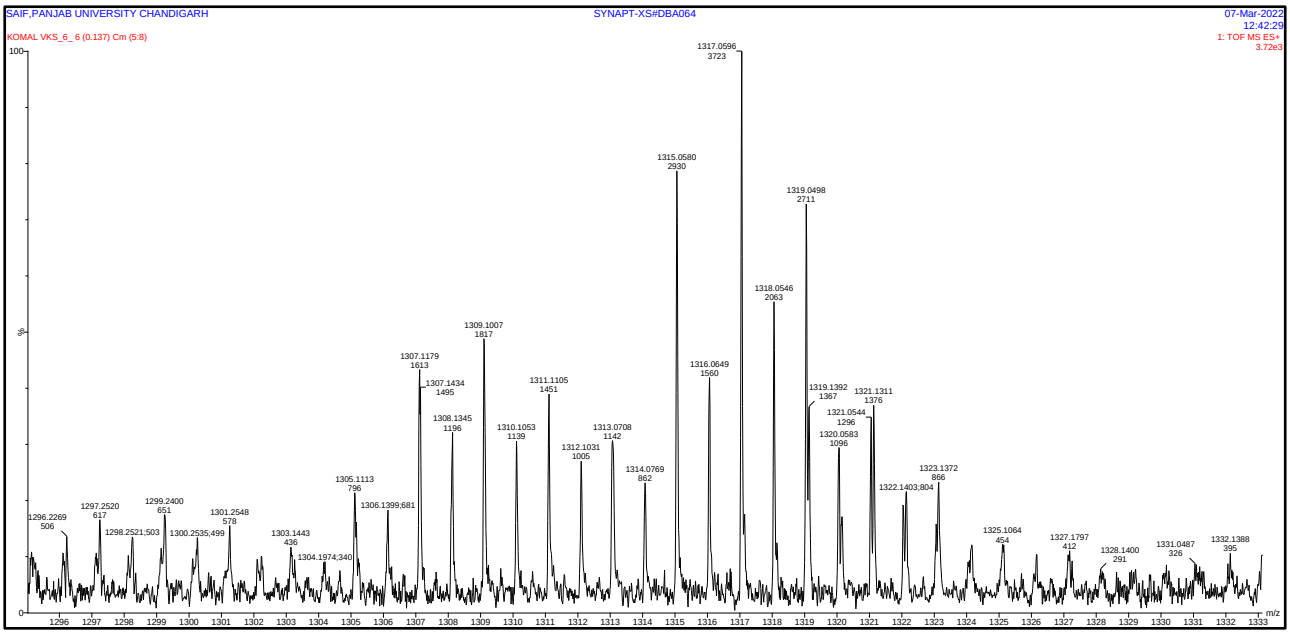

Annexure 3. HRMS spectrum of Complex **16**.

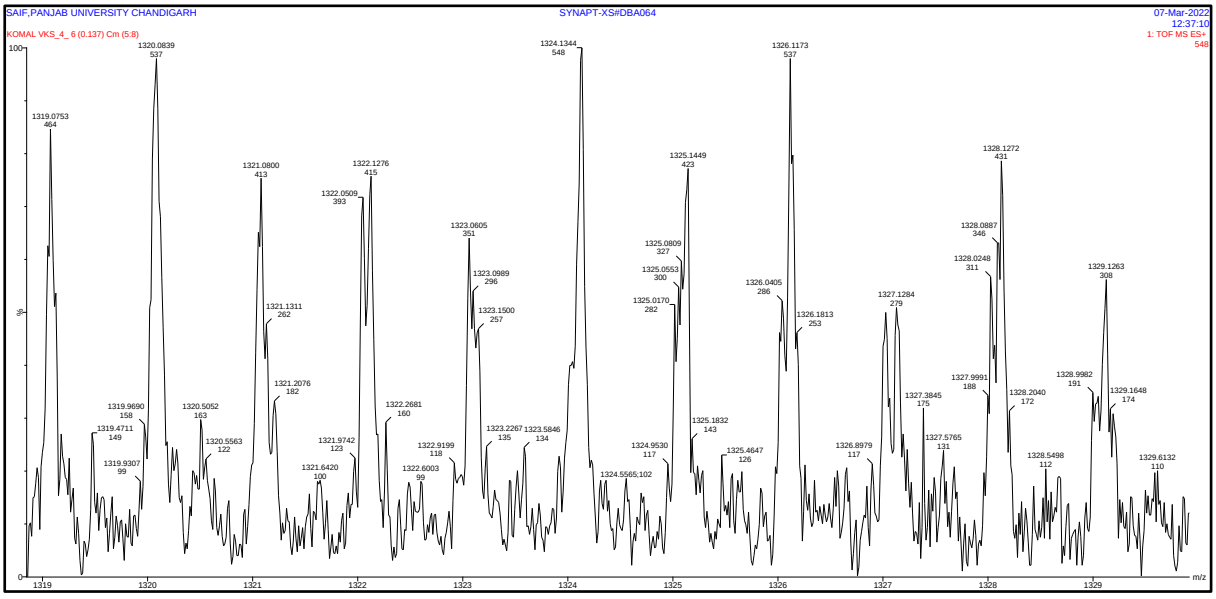

Annexure 4. HRMS spectrum of Complex **17**.

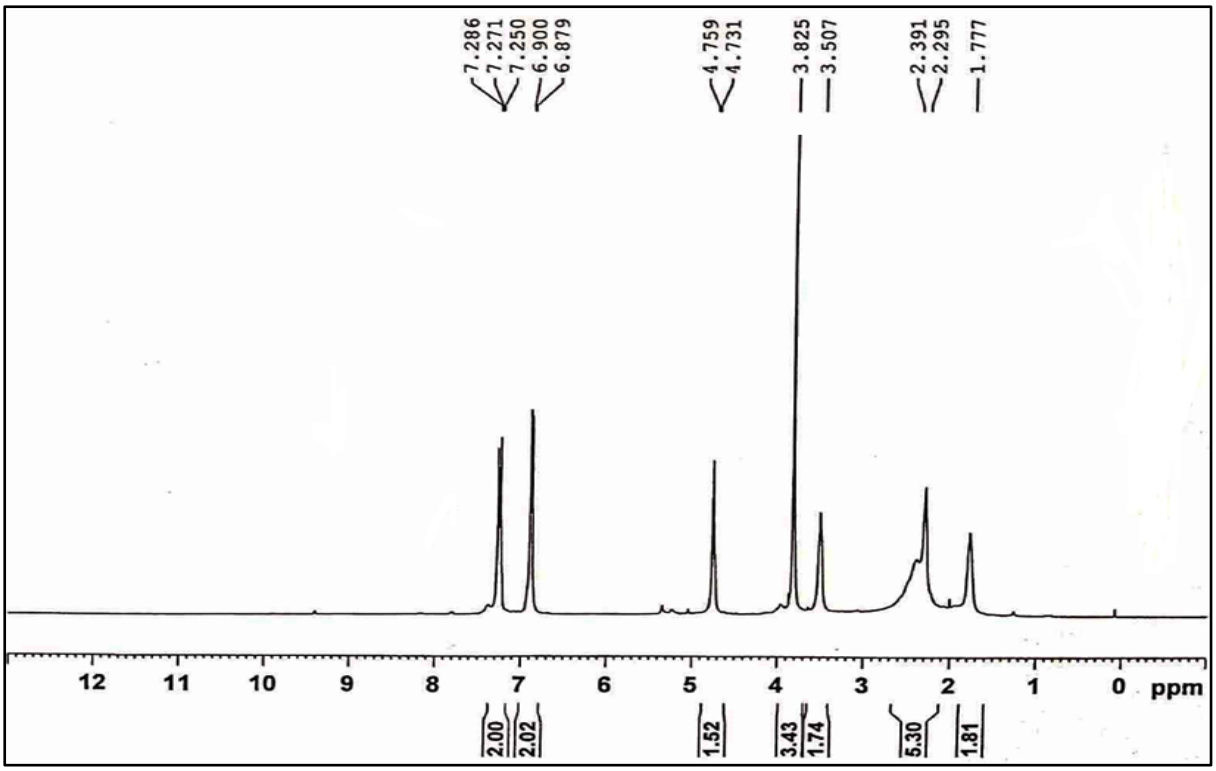

Annexure 5. ^{1}H NMR spectrum of complex **13**.

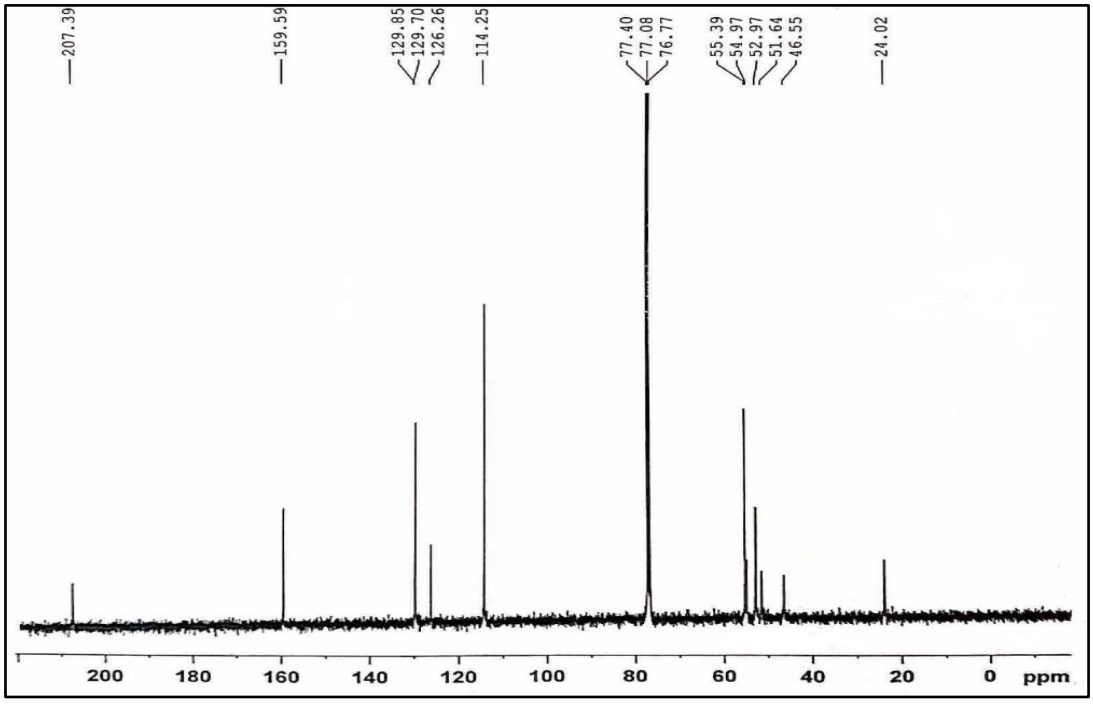

Annexure 6. ^{13}C NMR spectrum of complex **13**.

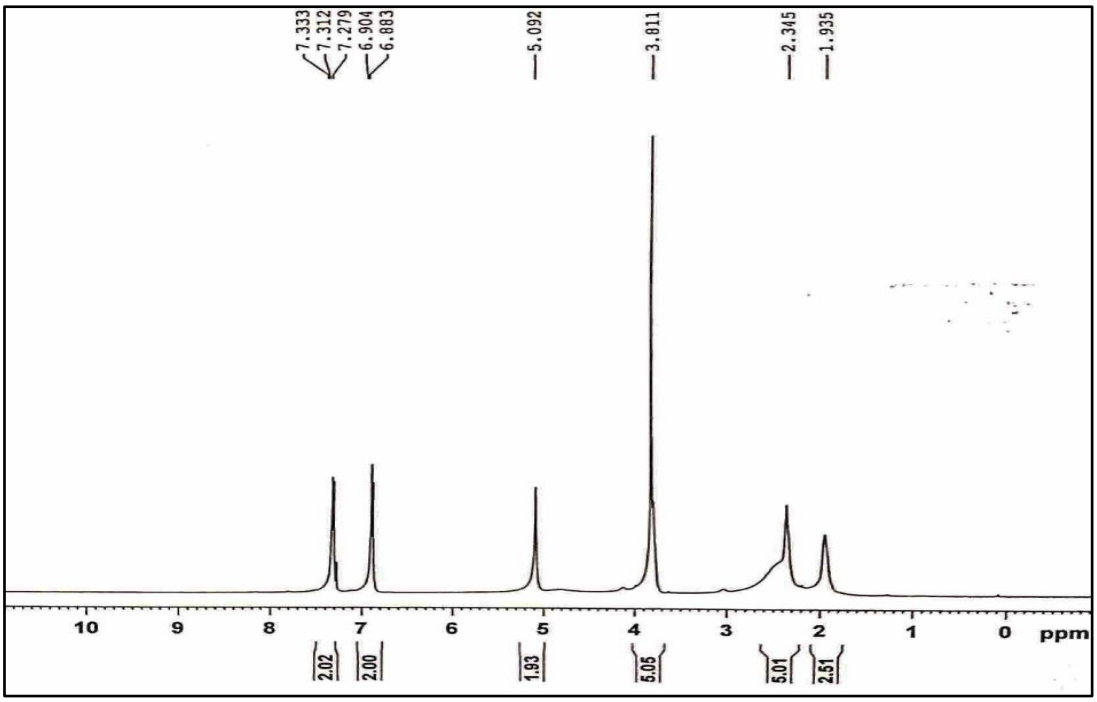

Annexure 7. ^{1}H NMR spectrum of complex **15**.

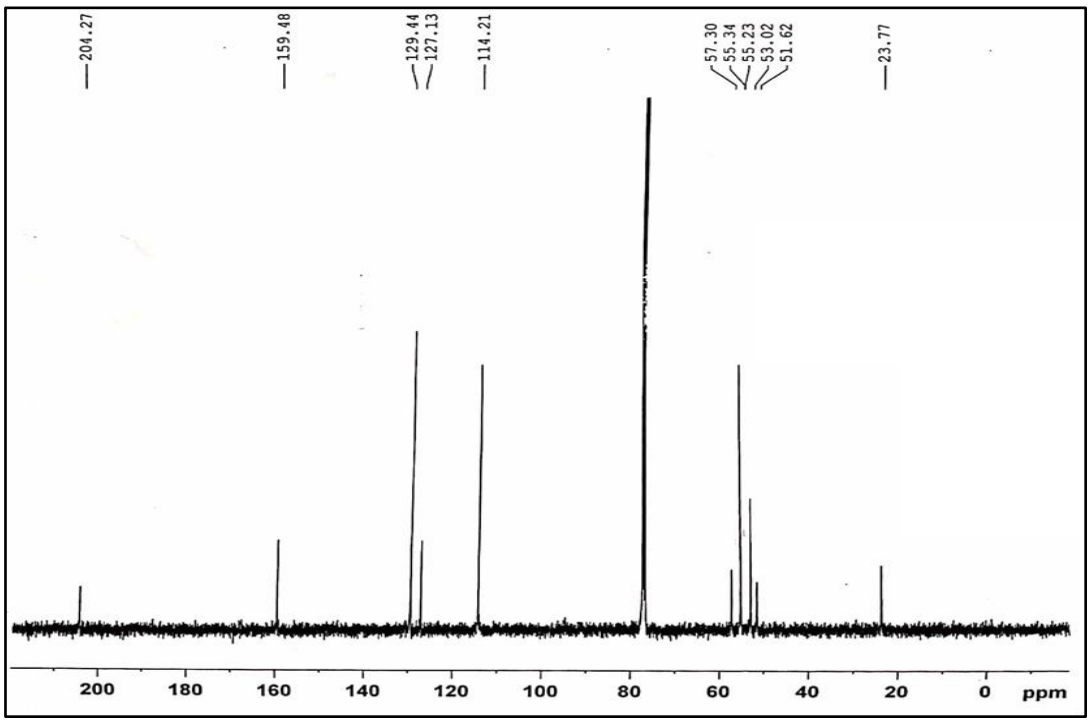

Annexure 8. ^{13}C NMR spectrum of complex **15**.

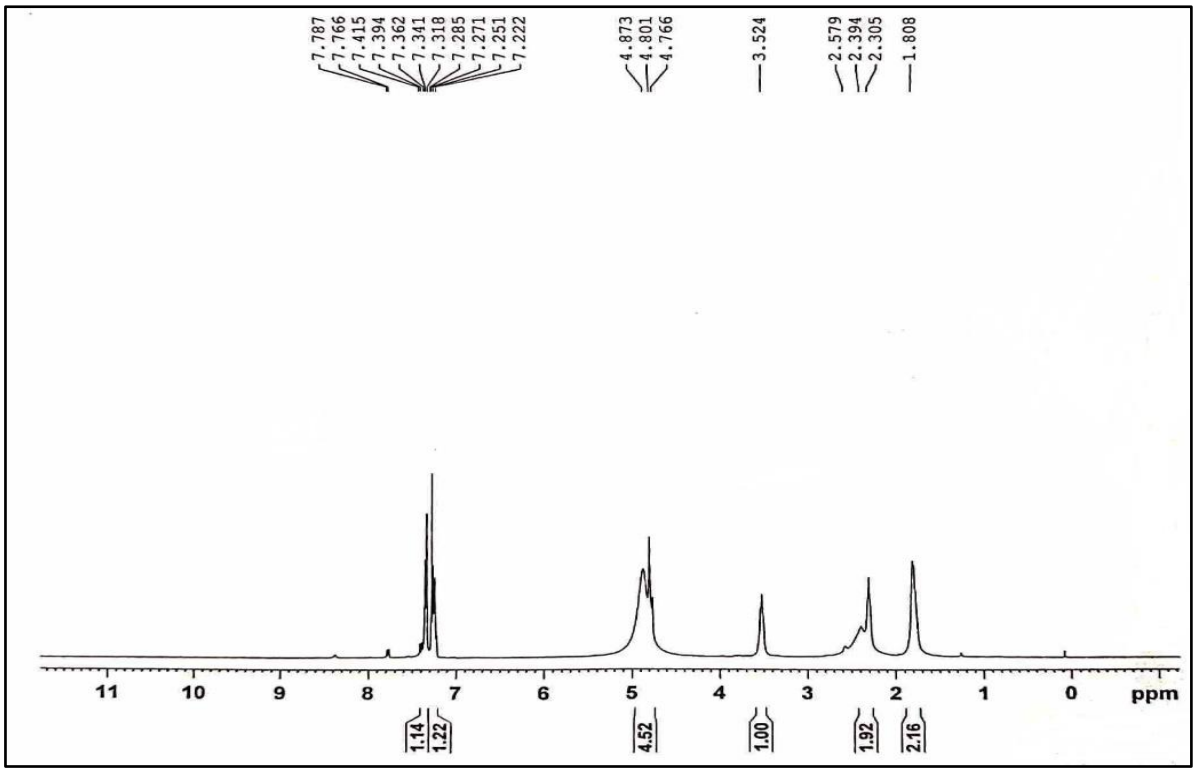

Annexure 9. ^{1}H NMR spectrum of complex **16**.

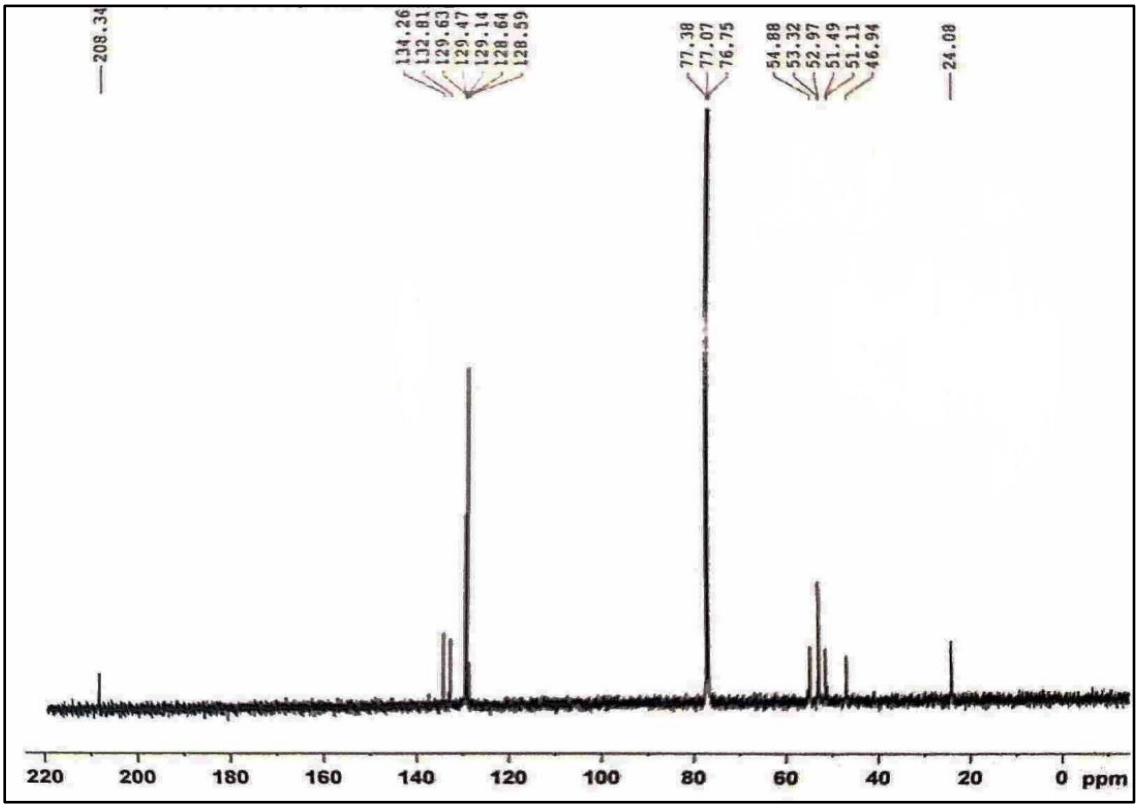

Annexure 10. ^{13}C NMR spectrum of complex **16**.

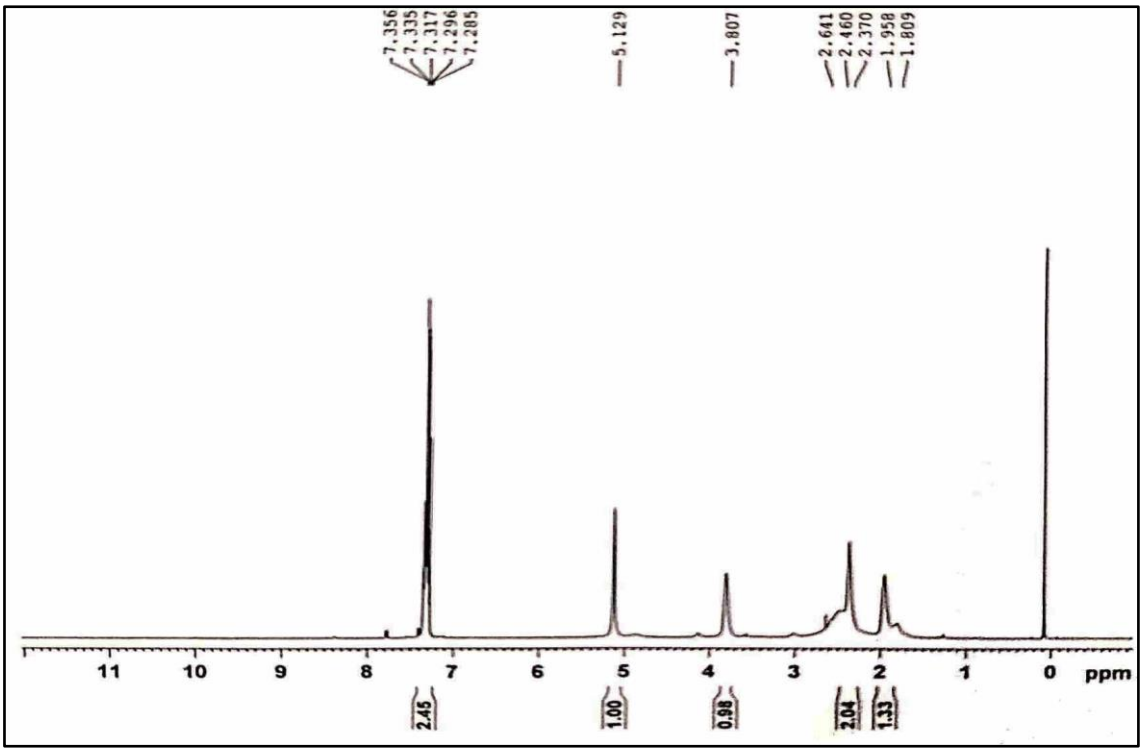

Annexure 11. ^{1}H NMR spectrum of complex **18**.

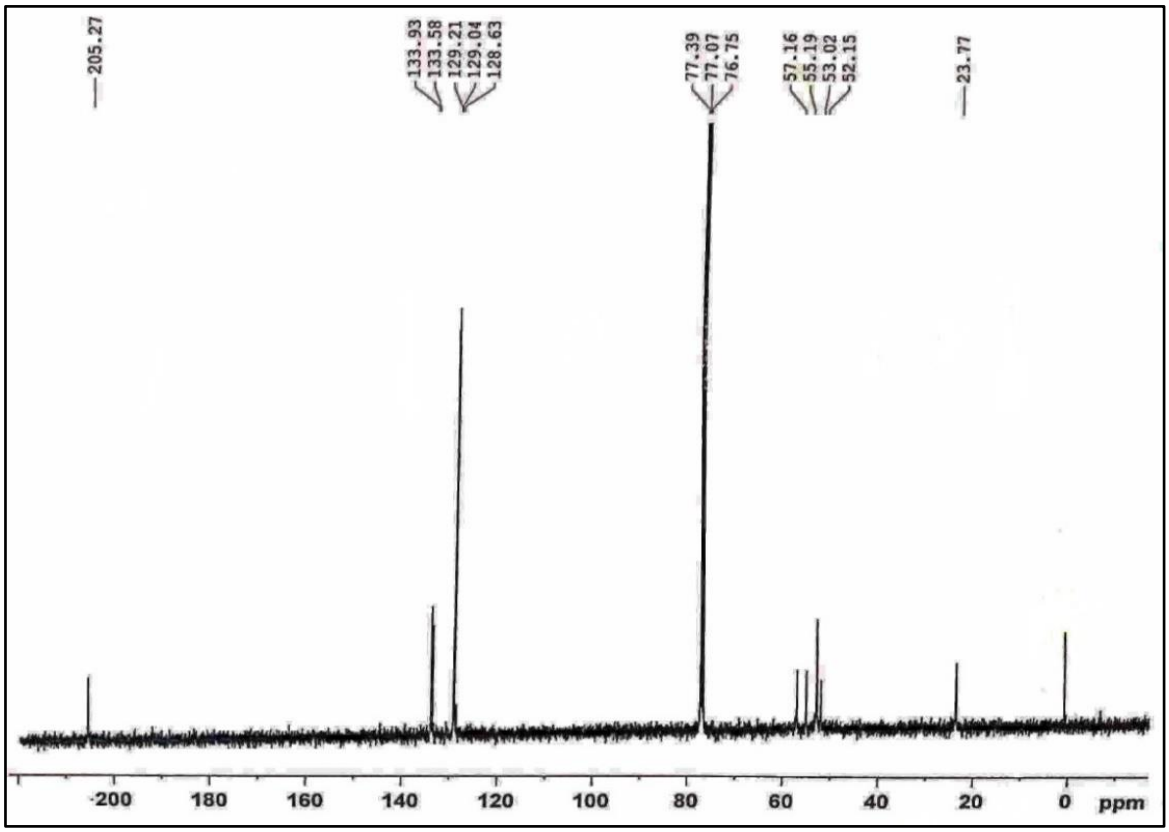

Annexure 12. ^{13}C NMR spectrum of complex **18**.

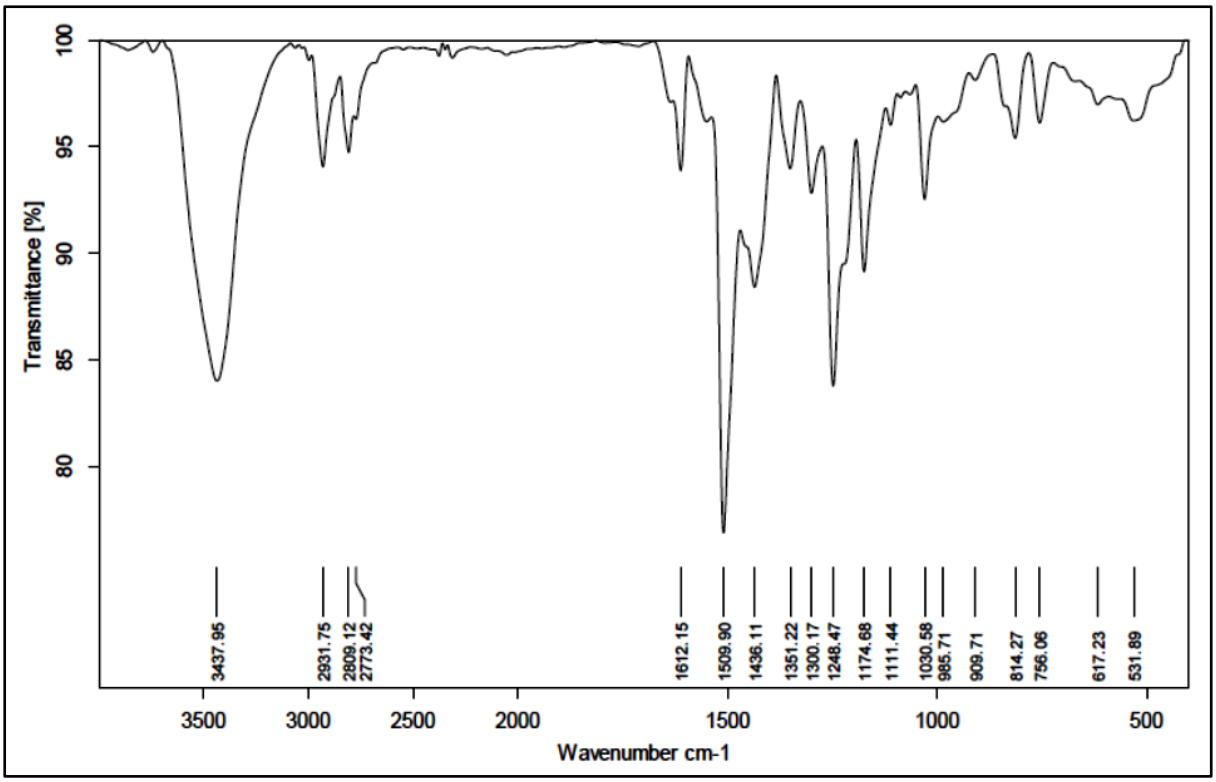

Annexure 13. FTIR spectrum of Complex **13**.

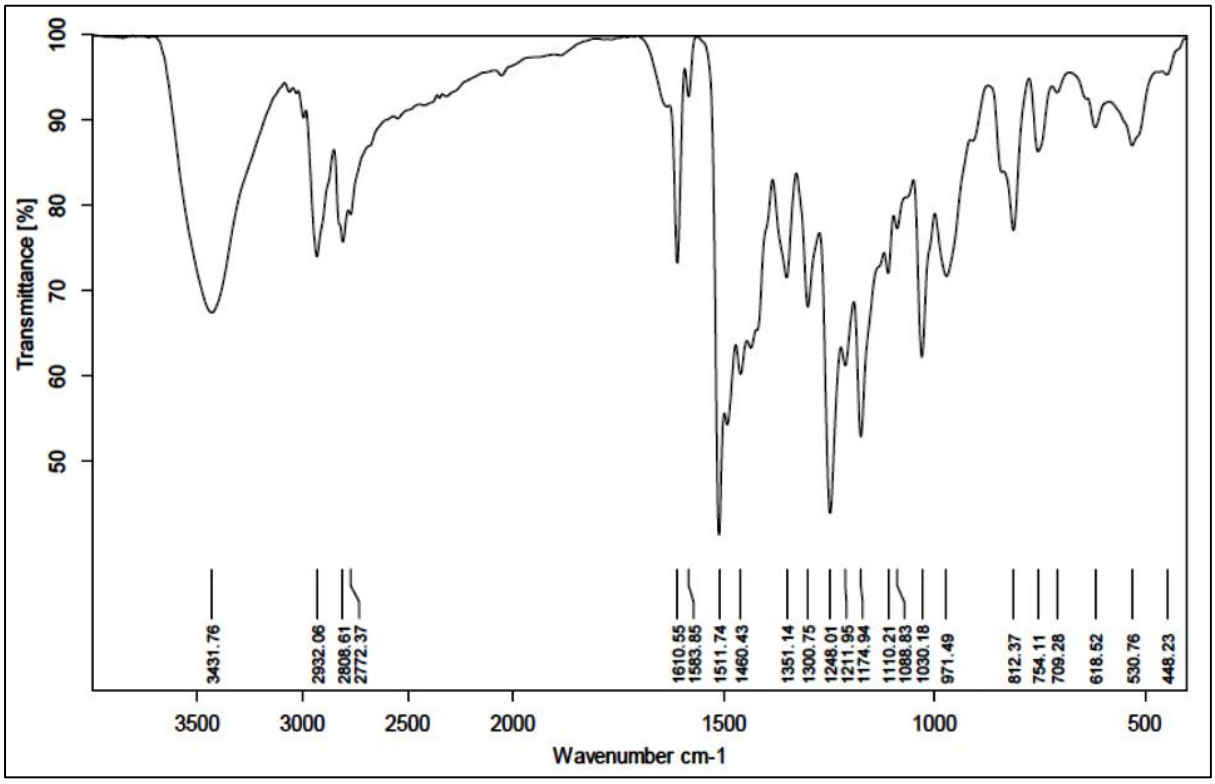

Annexure 14. FTIR spectrum of Complex **14**.

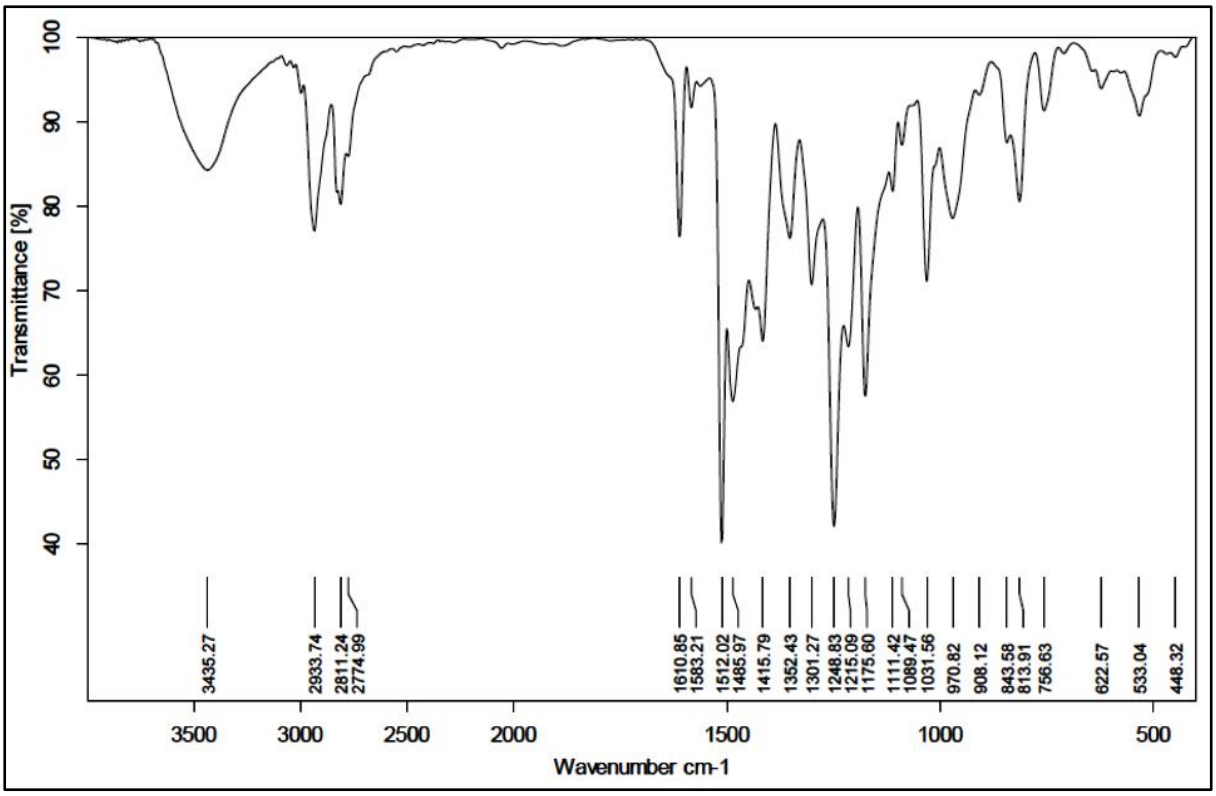

Annexure 15. FTIR spectrum of Complex **15**.

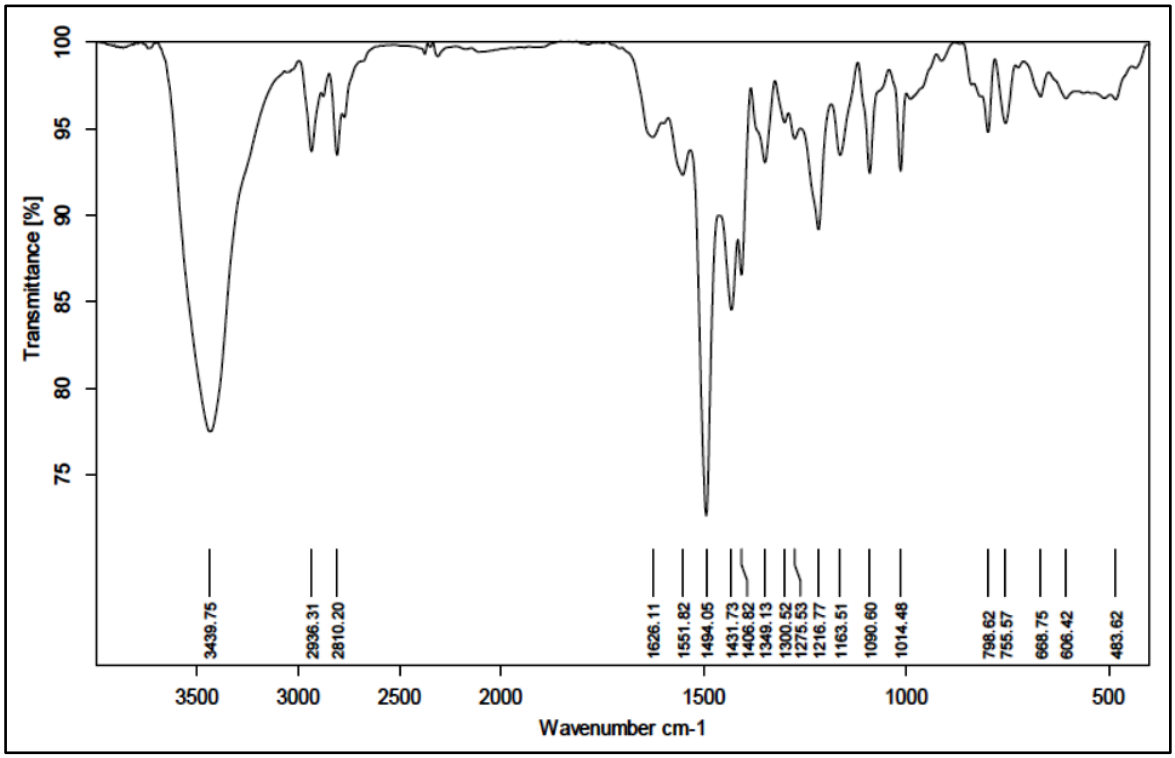

Annexure 16. FTIR spectrum of Complex **16**.

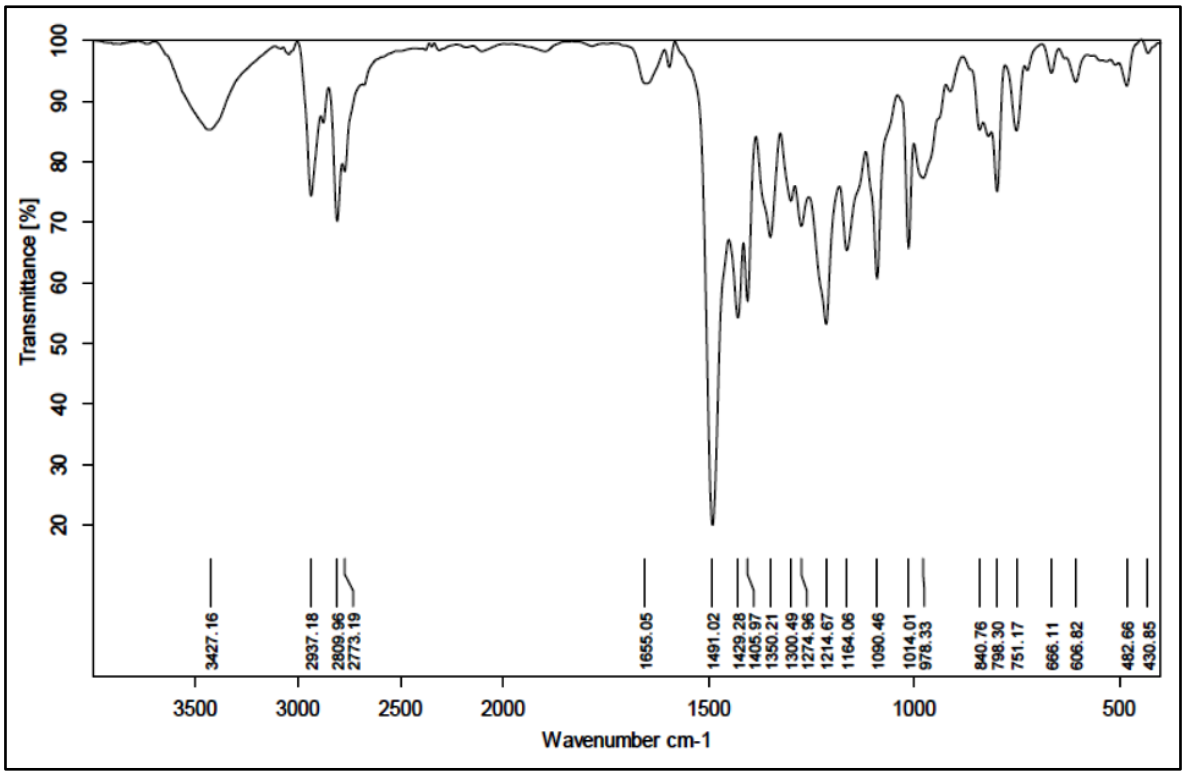

Annexure 17. FTIR spectrum of Complex **17**.

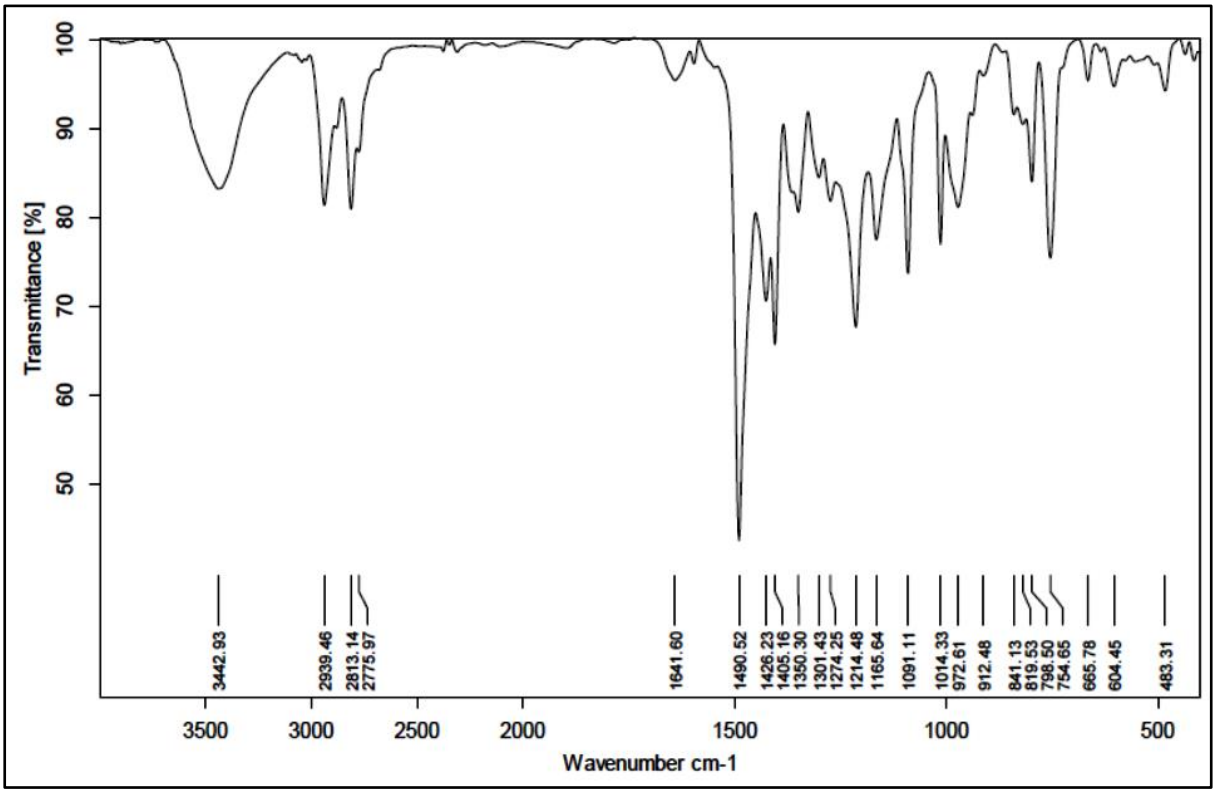

Annexure 18. FTIR spectrum of Complex **18**.